

# THE PRECAMBRIAN PALEOGEOGRAPHY OF LAURENTIA

Nicholas L. Swanson-Hysell

Department of Earth and Planetary Science, University of California, Berkeley, CA 94720 USA

## ABSTRACT

Laurentia is the craton that forms the Precambrian core of North America and was a major continent throughout the majority of the Proterozoic following its ca. 1.8 Ga amalgamation. The paleogeographic position of Laurentia is key to the development of reconstructions of Proterozoic paleogeography including the Paleoproterozoic to Mesoproterozoic supercontinent Nuna and latest Mesoproterozoic to Neoproterozoic supercontinent Rodinia. There is a rich record of Precambrian paleomagnetic poles from Laurentia, as well as an extensive and well-documented geologic history of tectonism. These geologic and paleomagnetic records are increasingly better constrained geochronologically and are both key to evaluating and developing paleogeographic models. These data from Laurentia provide strong support for mobile lid plate tectonic processes operating continuously over the past 2.2 billion years.

*This manuscript is a preprint of the chapter:*

Swanson-Hysell, N. L. (2021) Chapter 4: The Precambrian paleogeography of Laurentia. In: Pesonen, L.J., Salminen, J., Evans, D.A.D., Elming, S.-., Veikkolainen, T. (eds.) *Ancient Supercontinents and the Paleogeography of the Earth*.

## 4.1 INTRODUCTION AND BROAD TECTONIC HISTORY

LAURENTIA refers to the craton that forms the Precambrian interior of North America and Greenland (Fig. 1). Laurentia comprises multiple Archean provinces that had unique histories prior to their amalgamation in the Paleoproterozoic (ca. 1.8 Ga), as well as tectonic zones of crustal growth that post-date this assembly (Whitmeyer and Karlstrom, 2007). Collision between the Superior province and the composite Slave+Rae+Hearne provinces that resulted in the Trans-Hudson orogeny represents a major event in the formation of Laurentia (Corrigan et al., 2009). Terminal collision recorded in the Trans-Hudson orogen is estimated to have been ca. 1.86 to 1.82 Ga based on constraints such as U-Pb dating of monazite grains and zircon rims (Skipton et al., 2016; Weller and St-Onge, 2017). A period of accretionary and collisional orogenesis is recorded in the constituent provinces and terranes of Laurentia leading up to the terminal collision of the Trans-Hudson orogeny. This overall story of rapid Paleoproterozoic amalgamation of Laurentia's constituent Archean provinces, including the terminal Trans-Hudson orogeny, was synthesized in the seminal *United Plates of America* paper of Hoffman (1988) and has been refined in the time since – particularly with additional geochronological constraints. Of most relevance here are the events that led to the suturing of more major Archean provinces: the Thelon orogen associated with the collision between the Slave and Rae provinces ca. 2.0 to 1.9 Ga (?); the Snowbird orogen associated with ca. 1.90 Ga collision between the Rae and Hearne provinces and associated terranes (Berman et al., 2007; Thiessen et al., 2020); the Nagssugtoqidian orogen due to the ca. 1.86 to 1.84 Ga collision between the Rae and North Atlantic provinces (St-Onge et al., 2009); and the Torngat orogen resulting from the ca. 1.87 to 1.85 Ga collision of the southern Meta Incognita province (grouped with the Rae province in older compilations) with the North Atlantic province (St-Onge et al., 2009).

As for the suturing of the Wyoming province to Laurentia, many models posit that it was conjoined with Hearne and associated provinces at the time of the Trans-Hudson orogeny

(e.g. St-Onge et al., 2009; Pehrsson et al., 2015) or was proximal to the Hearne and Superior provinces while still undergoing continued translation up to ca. 1.80 Ga (Whitmeyer and Karlstrom, 2007). A contrasting view has been proposed that the Wyoming and Medicine Hat provinces were not conjoined with the other Laurentia provinces until ca. 1.72 Ga (Kilian et al., 2016). This interpretation is argued to be consistent with geochronological constraints on monazite and metamorphic zircon indicating active collisional orogenesis associated with the Big Sky orogen on the northern margin of the craton as late as ca. 1.75 to 1.72 Ga (Condit et al., 2015) and ca. 1.72 tectonomagmatic activity in the Black Hills region (Redden et al., 1990). However, the evidence for earlier orogenesis ca. 1.78 to 1.75 in the Black Hills (Dahl et al., 1999; Hrncir et al., 2017), as well as high-grade metamorphism as early as ca. 1.81 Ga in the Big Sky orogen (Condit et al., 2015), may support the interpretation of Hrncir et al. (2017) that ca. 1.72 Ga activity is a minor overprint on ca. 1.75 terminal suturing between the Wyoming and Superior provinces. Regardless, in both of these interpretations, Wyoming is a later addition to Laurentia with final suturing post-dating ca. 1.82 Ga amalgamation of Archean provinces with the Trans-Hudson orogen further to the northeast. Overall, the collision of these Archean microcontinents between ca. 1.9 and 1.8 Ga led to rapid amalgamation of the majority of the Laurentia craton (Fig. 1).

Crustal growth also progressed in the Paleoproterozoic through accretionary orogenesis. This accretion occurred within the Wopmay orogen through ca. 1.88 Ga arc-continent collision that led to the accretion of the Hottah terrane (the Calderian orogeny) and the subsequent emplacement of the Great Bear magmatic zone from ca. 1.88 to 1.84 Ga (Hildebrand et al., 2009). Coeval with the Trans-Hudson orogeny was the peripheral Penokean orogeny during which both microcontinent blocks (the Marshfield terrane) and arc terranes accreted on the southeastern margin of the west Superior province ca. 1.86 to 1.82 (Schulz and Cannon, 2007). Firm evidence of the end of the orogeny comes from the ca. 1.78 undeformed plutons of the post-Penokean East Central Minnesota Batholith (Holm et al., 2005).

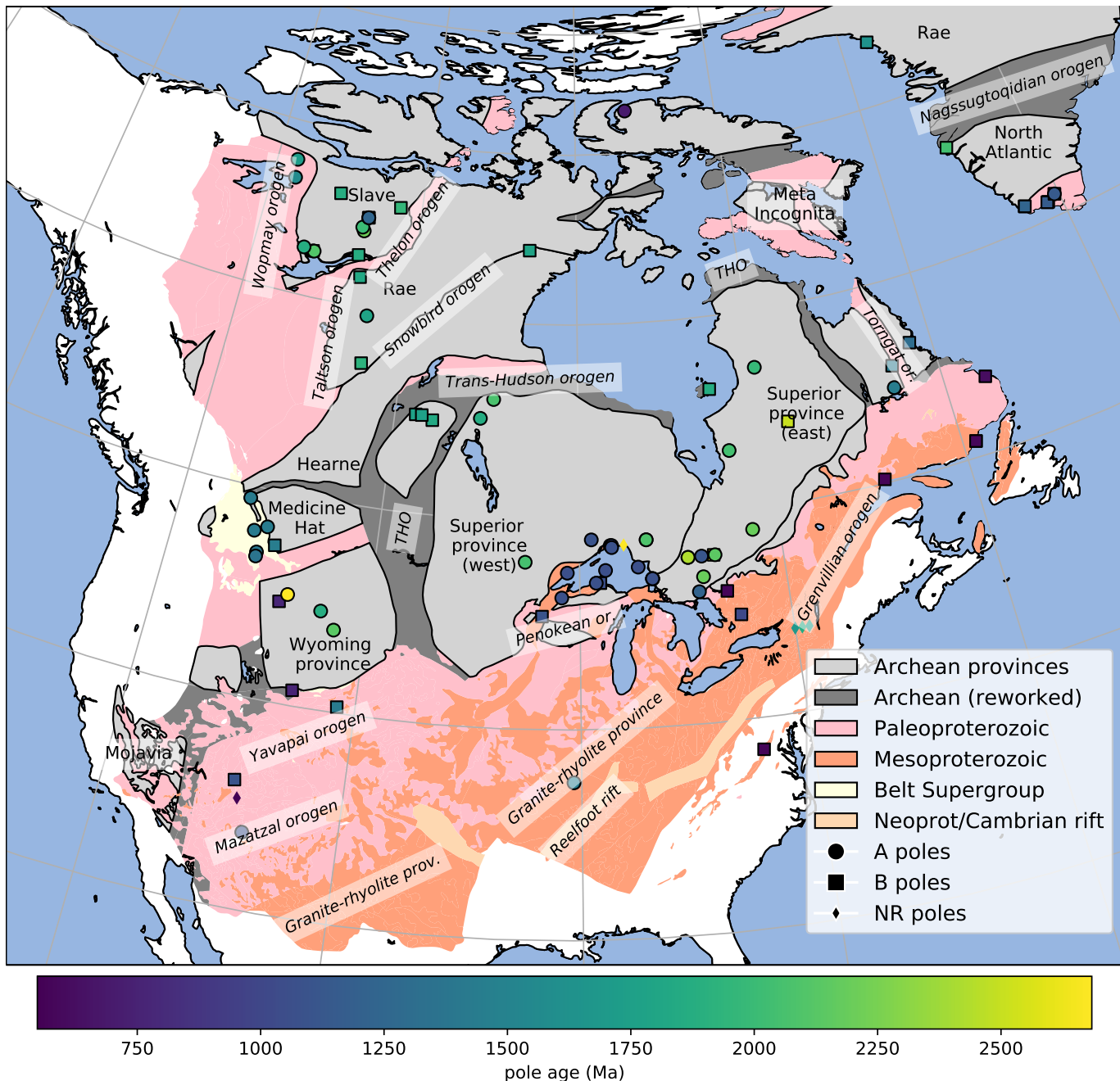


**Figure 1: Simplified map of the tectonic units of Laurentia.** The location of Archean provinces (labeled with text) and younger Paleoproterozoic and Mesoproterozoic crust are simplified from Whitmeyer and Karlstrom (2007) with additions for Greenland based on St-Onge et al. (2009). Proterozoic orogens are labeled with *italicized* text (or. – orogen; THO – Trans-Hudson orogen; prov. – province). The localities from which the compiled Precambrian paleomagnetic poles were developed are shown and colored by age. The circles (A rated poles) and squares (B rated poles) have been assessed by the Nordic workshop panel (Evans et al., 2021).

The collisions of provinces and terranes leading up to the Trans-Hudson orogeny mark the initial phase of assembly of the supercontinent Nuna in the paleogeographic model framework of Pehrsson et al. (2015). The Trans-Hudson orogeny itself is taken to be the terminal collision associated with the closure of the Manikewan Ocean that had previously been a large oceanic tract separating the Superior province from the composite Slave+Rae+Hearne+North Atlantic provinces (often referred to as the Churchill domain or plate; e.g. Skipton et al., 2016; Weller and St-Onge, 2017; Fig. 4). The paleogeographic mode of Pehrsson et al. (2015) posits that this period of terminal collision not only resulted in the amalgamation of Laurentia, but was also associated with the assembly of the supercontinent Nuna that is hypothesized to include other major Paleoproterozoic cratons including Baltica, Siberia, Congo, São Francisco, West Africa, and Amazonia. In this volume, Elming et al. (2021) put forward an alternate scenario for Nuna paleogeography. In their model, Laurentia, Baltica and Siberia become conjoined at the time of Laurentia amalgamation forming the core of Nuna (as in Evans and Mitchell, 2011). This core then subsequently grows to be a semi-supercontinent with India and Australia, however Amazonia, West Africa, Congo and São Francisco cratons remain independent from Nuna.

Following the Trans-Hudson orogeny, the locus of orogenesis migrated to the exterior of Laurentia. This change marks a shift in the predominant style of Laurentia's growth as subsequent crustal growth occurred dominantly through accretion of juvenile crust along the southern and eastern margin of the nucleus of Archean provinces (Whitmeyer and Karlstrom, 2007; Figs. 1 and 2). Determining the extent of these belts is complicated by poor exposure of them in the midcontinent relative to the exposure of the Archean provinces throughout the Canadian shield. Major growth of Laurentia following the amalgamation of these Archean provinces occurred associated with the arc-continent collision of the ca. 1.71 to 1.68 Ga Yavapai orogeny (Fig. 2). Yavapai orogenesis is interpreted to have resulted from the accretion of a series of arc terranes that collided with each other and Laurentia (Karlstrom et al., 2001). Yavapai accretion was followed by widespread emplacement of granitoid intrusions (Whitmeyer and Karlstrom, 2007). These intrusions are hypothesized to have stabilized the juvenile accreted terranes that subsequently remained part of Laurentia (Whitmeyer and Karlstrom, 2007). Subsequent accretionary orogenesis of the ca. 1.65 to 1.60 Ga Mazatzal orogeny and associated plutonism led to further crustal growth in the latest Paleoproterozoic (Karlstrom and Bowring, 1988). Laurentia's growth continued in the Mesoproterozoic along the southeast margin through further juvenile terrane and arc accretion. An interval of major plutonism occurred ca. 1.48 to 1.35 Ga leading to the formation of A-type granitoids throughout both Mesoproterozoic and Paleoproterozoic provinces extending from the southwest United States up to the Central Gneiss Belt of Ontario to the northeast of Georgian Bay (Slagstad et al., 2009). This plutonism is interpreted to be associated with a combination of continental arc magmatism and melt generation within a back-arc region Laurentia's long-live active margin (Bickford et al., 2015). Metamorphic rocks from Mesoproterozoic sedimentary and volcanic protoliths in northern New Mexico have been interpreted to indicate an interval of ca. 1.46 to 1.40 Ga orogenesis that has been named the Picuris orogeny (Daniel et al., 2013; Aronoff et al.,

2016). Younger magmatic activity ca. 1.37 Ga of the Southern Granite-Rhyolite Province suggests a similar active margin setting at that time (Bickford et al., 2015). While an active margin interpretation for the Granite-Rhyolite Province with arc and back-arc magmatism in a back-arc setting has gained traction within the literature, the tectonic setting is often described as enigmatic given earlier interpretations of an anorogenic setting (see references in Slagstad et al., 2009).

Accretionary orogenesis continued along the eastern margin of Laurentia with the amalgamation and accretion of arcs associated with the ca. 1.25 to 1.22 Ga Elzevirian orogeny (McLelland et al., 2013). The subsequent ca. 1.19 to 1.16 Ga Shawinigan orogeny is interpreted to be due to the collision of terrane comprised of a previously rifted fragment of Laurentia and led to obduction of the Pyrites Complex ophiolite (McLelland et al., 2010; Chiarenzelli et al., 2011). The Shawinigan orogeny is followed by a period of tectonic quiescence on the eastern margin of Laurentia until the collisional orogenesis of the Grenvillian orogeny (McLelland et al., 2010). An exception to this quiescence during the interval between the Shawinigan and Grenvillian orogenies is ca. 1.15 to 1.12 Ga orogenesis in the Llano uplift of the southern Laurentia margin (Mosher, 1998). Llano orogenesis is interpreted to have resulted from collision of continental lithosphere along with an accreted arc (Mosher, 1998). This orogenesis is earlier and temporally distinct from the Grenvillian orogeny, is only known from a limited spatial area, and is located in a region that experienced further orogenesis during the Grenvillian orogeny (Grimes and Copeland, 2004). Taken together, this context is suggestive of a microcontinent collision leading to Llano uplift orogenesis prior to terminal Grenvillian continental collision. If this interpretation is correct, it is similar to Paleozoic orogenesis along the margin where microcontinent collision resulted in the Acadian orogeny prior to Alleghanian orogenesis during the Appalachian orogenic interval (2).

The Grenvillian orogeny was a protracted interval of continent-continent collision (ca. 1.09 to 0.98 Ga) leading to amphibolite to granulite facies metamorphism through the orogen (McLelland et al., 2010). Evidence of large-scale continent-continent collision at the time of the Ottawa Phase of the Grenvillian orogeny is recorded in Texas (Grimes and Copeland, 2004), up through the Blue Ridge Appalachian inliers (Johnson et al., 2020), through Ontario and up to the Labrador Sea (Rivers, 2008). The orogeny is interpreted to have resulted in the development of a thick plateau associated with the Ottawa orogenic phase (ca. 1090 to 1030 Ma; Rivers, 2008). Continued convergence during the Rigolet phase of the Grenvillian orogeny led to the development of the Grenville Front tectonic zone and ended ca. 980 Ma (Hynes and Rivers, 2010).

In the latest Mesoproterozoic (ca. 1.11 to 1.08 Ga) prior to the Grenvillian orogeny, a major intracontinental rift co-located with a large igneous province formed in Laurentia's interior leading to extension within the Archean Superior province and adjacent Paleoproterozoic provinces to the south (Cannon, 1992). This Midcontinent Rift led to the formation of a thick succession of volcanics and mafic intrusions that are well-preserved in Laurentia's interior. Midcontinent Rift development ceased as major collisional orogenesis of the Grenvillian orogeny began (Swanson-Hysell et al., 2019).

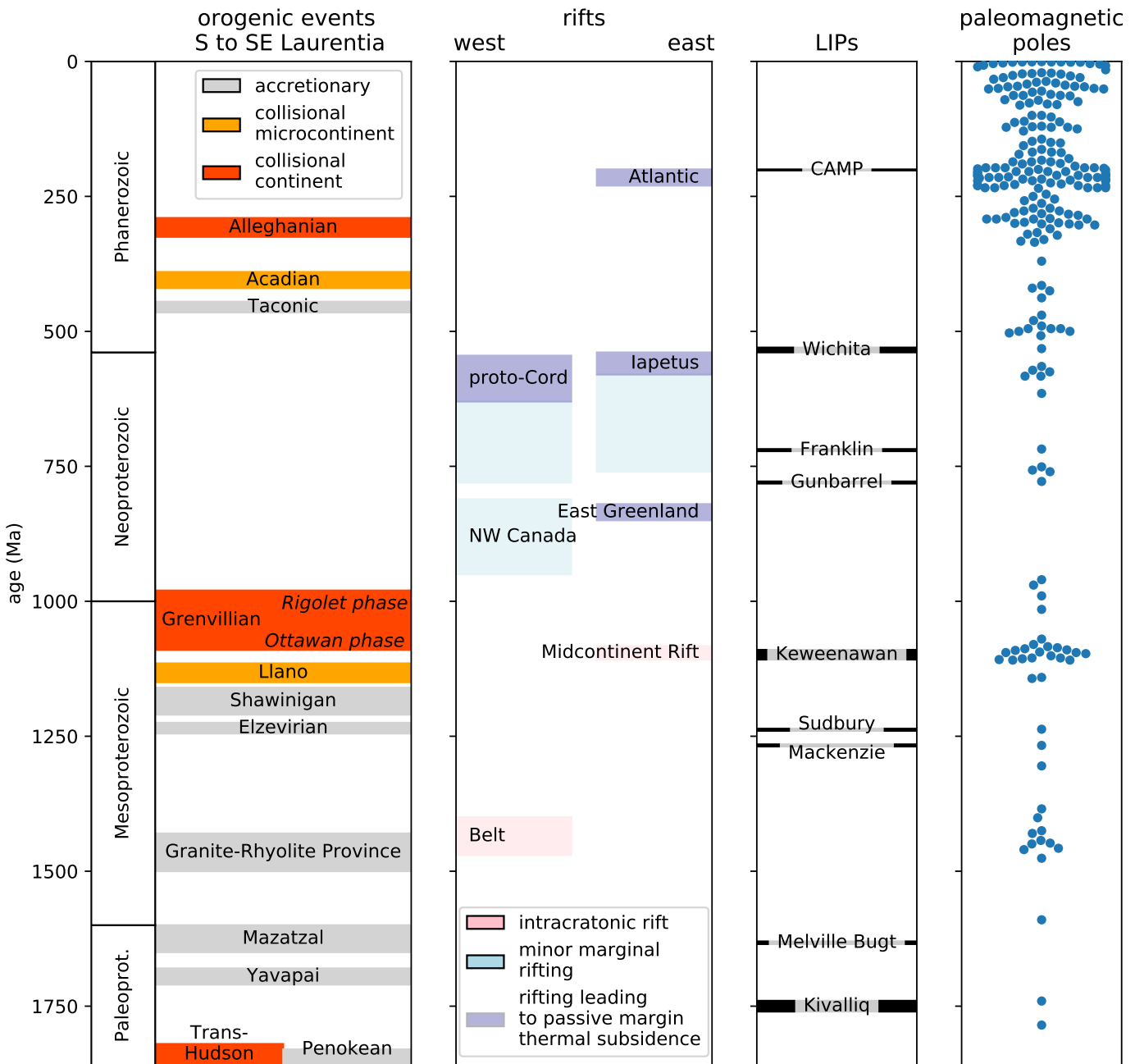


Figure 2: Simplified timeline of Laurentia's tectonic history over the past ~1.8 billion years. Brief summaries and references related to the orogenic and rifting episodes are given in the text. A timeline of large igneous provinces (LIPs) associated with typically brief and voluminous (or interpreted to be voluminous) volcanism is also shown. The interpreted age of paleomagnetic poles for Laurentia (not including separated terranes) compiled in this study for the Proterozoic and in Torsvik et al. (2012) for the Phanerozoic is shown. Abbreviations on the figure: CAMP (Central Atlantic Magmatic Province); proto-Cord (proto-Cordilleran).

There is significantly less preserved Mesoproterozoic crustal growth on the western margin of Laurentia (Fig. 1), and the tectonic history through the Mesoproterozoic Era is not as well elucidated as on the southern to eastern margin. The 15 to 20 km thick package of sedimentary rocks of the Belt-Purcell Supergroup is associated with a ca. 1.47 to 1.40 rift (Evans et al., 2000). While the rift is typically interpreted as being intracontinental (Lydon, 2004), the tectonic setting in which it formed is debated. ? proposed that it may be a remnant back-arc basin trapped within a continent, while others envision it as being associated with continental rifting along the margin associated with separation of a conjugate continent (Jones et al., 2015). This region is interpreted to have been subsequently deformed during a ca. 1.36 to 1.33 Ga event known as the East Koote-  
nay orogeny (McMechan and Price, 1982; Nesheim et al., 2012; McFarlane, 2015).

This late Paleoproterozoic and Mesoproterozoic tectonic history provides significant constraints on paleogeographic reconstructions. In particular, the long-lived history of accretionary orogenesis along the southeast (present-day coordinates) of Laurentia from the initiation of the Yavapai orogeny (ca. 1.71 Ga) to the end of the Shawinigan orogeny (ca. 1.16 Ga) requires a long-lived open margin without a major conjugate continent until the time of terminal Grenvillian collisional orogenesis (Karlstrom et al., 2001). This constraint is incorporated into models such as that of Zhang et al. (2012) and Pehrsson et al. (2015) which maintain a long-lived convergent margin throughout the Mesoproterozoic, but in some reconstructions other continental blocks are reconstructed into positions that are seemingly incompatible with this record of accretionary orogenesis (e.g. Amazonia in Elming et al., 2009, 2021). The high-grade metamorphism associated with the Ottawan phase of the Grenvillian orogeny itself strongly suggests a collision between Laurentia and (an)other continent(s) ca. 1080 Ma – the geological observation of which first led to the formulation of the hypothesis of the supercontinent Rodinia (Hoffman, 1991). This extensive and major collisional orogenic history recorded in Laurentia, and also present on other Proterozoic continents, at this time remains a strong piece of evidence that a supercontinent or (proto)supercontinent formed at the 1.0 Ga Mesoproterozoic to Neoproterozoic transition. Note that while the term Grenville orogeny or Grenville belt is used rather loosely throughout much of the literature to refer to any late Mesoproterozoic orogenic belt, the timeline of orogenesis on the Laurentia margin has more nuanced constraints than this usage. These constraints can be comparatively assessed when evaluating potential conjugate continents to Laurentia associated with the orogen (Fig. 2).

The subsequent Neoproterozoic tectonic history of Laurentia is dominantly a record of rifting (Fig. 2). Along the western margin of Laurentia, rifting occurred ca. 780 to 720 Ma leading to deposition in basins from the Death Valley region of SW Laurentia to the Mackenzie Mountains of NW Laurentia (Macdonald et al., 2013; Dehler et al., 2017; Rooney et al., 2017). However, this extensional basin development predates the rifting that led to well-documented passive margin thermal subsidence closer to the ca. 539 Ma Neoproterozoic-Phanerozoic boundary (Bond et al., 1984; Levy and Christie-Blick, 1991). The emplacement of the ca. 780 Ma Gunbarrel large igneous province along this margin and the subsequent extension recorded in the

basins is commonly interpreted to be associated with the break-up of Laurentia and a conjugate continent to the western margin (often interpreted to be Australia). If this interpretation is correct, it is unclear why there would be minimal thermal subsidence until the Ediacaran (post 635 Ma as in Levy and Christie-Blick, 1991 and Witkosky and Wernicke, 2018). The geological evidence therefore supports prolonged active tectonism along the western margin of Laurentia (a portion of which could be strike-slip and transtensional; Smith et al., 2015), but suggests that there was significant lithospheric thinning associated with rifting later than the timing of rifting typically implemented in models of Rodinia break-up. The record of Neoproterozoic basin development led Yonkee et al. (2014) to propose that the early ca. 780 Ma rifting was intracratonic and that while it may have led to some associated thermal subsidence that there was a second interval of rifting and thermal subsidence associated with Australia rifting away in the Ediacaran (later than in most models). Another possibility, along the lines of that proposed in Ross (1991), is that ca. 780 Ma extensional tectonism is an inboard record of rifting and passive margin development that occurred further outboard. In this model, subsequent continent rifting that drove lithospheric thinning, perhaps associated with the departure of a microcontinent fragment rather than an already departed major conjugate continent, would be the cause of Ediacaran to Cambrian thermal subsidence.

In northwest Laurentia from the Ogilvie Mountains of Yukon to Victoria Island, the sedimentary rock record is distinct from further south as it also records earlier Neoproterozoic basin development during the Tonian Period in addition to Cryogenian basin development (Macdonald et al., 2012). Tectonic extension is recorded in units of the lower Fifteenmile Group with maximum depositional ages of ca. 1050 Ma with ongoing basin development ca. 812 Ma (age constraint from a U-Pb zircon date on a tuff within the upper Fifteenmile Group; Macdonald et al., 2010) potentially through thermal subsidence (Macdonald et al., 2012). Earlier basin development in the region recorded by the Mesoproterozoic/Neoproterozoic Pinguicula Group could provide valuable insight on tectonic history as it has been interpreted to have been deposited in an extensional basin (Medig et al., 2016), however it is poorly constrained in terms of age – older than the Fifteenmile Group and younger than the ca. 1382 Ma Hart River sills (which themselves have been interpreted to be emplaced in conjunction with rifting; Verbaas et al., 2018).

Another margin that experienced rifting and associated passive margin thermal subsidence earlier in the Neoproterozoic is the northeast Greenland margin (Fig. 2). Available geochronological constraints and thermal subsidence modeling indicate ca. 850 to 820 Ma rifting followed by thermal subsidence of a stable platform (Maloof et al., 2006; Halverson et al., 2018). These data suggest that conjugate continental lithosphere had rifted away from northeast Greenland by ca. 820 Ma.

Extensive rifting followed by thermal subsidence occurred along the southeast to east Laurentia margin in the time leading up to the Neoproterozoic-Phanerozoic boundary and is interpreted to be associated with the opening of the Iapetus ocean. A record of this rifting is preserved as rift basins that were part of failed arms (Rome trough, Reelfoot rift and Oklahoma aulacogen; Fig. 1) as well as prolonged Cambrian to Ordovician pas-

sive margin thermal subsidence along the margin (Bond et al., 1984; Whitmeyer and Karlstrom, 2007). The age of igneous intrusions that have been interpreted to be rift-related play a significant role in interpretations of this history such as in the rift development model of Burton and Southworth (2010). In this model, spatially-restricted rifting occurs ca. 760 to 680 Ma in the region of modern-day North Carolina and Virginia. Rifting ca. 620 to 580 Ma initiates in the region from modern-day New York to Newfoundland and by ca. 580 to 550 Ma rifting extends along the length of Laurentia's eastern margin. The last phase of this rifting has been interpreted to be associated with the separation of the Argentine pre-Cordillera Cuyania terrane (Dickerson and Keller, 1998). As with other rifts, it is difficult to distinguish the separation of a cratonic fragment as a micro-continent from the rifting and departure of a major craton, as the record that lingers on the craton is similar. Recognizing this ambiguity, Robert et al. (2020) propose that rather than being associated with spatially-restricted or failed rifting that ca. 700 Ma extension is associated with breakup and separation of Laurentia and its conjugate continent (that they interpret to be Amazonia). This rifting would have led to the formation of the Paleo-Iapetus Ocean (an analogue with the Paleo-Tethys). Subsequent to this rifting of the major continental blocks, smaller terranes of lithosphere rift off the east Laurentia margin ca. 600 Ma leading to the formation of the Neo-Iapetus Ocean and the record of passive margin development on Laurentia (Robert et al., 2020).

The eastern margin of Laurentia then went through the multiple phases of Appalachian orogenesis. As is visualized in Figure 2, there are parallels between the Grenville orogenic interval and the Appalachian orogenic interval in that there was a period of arc-continent collision (Elzevirian orogeny in the Grenville interval; Taconic orogeny in the Appalachian interval) followed by microcontinent accretion (Shawinigan/Llano orogenies in the Grenville interval; Acadian orogeny in the Appalachian interval) that culminated in large-scale continent-continent collision (Grenvillian orogeny in the Grenville interval; Alleghanian orogeny in the Appalachian interval). These similarities are the consequence of an active margin facing an ocean basin that was progressively consumed until continent-continent collision. In the case of the Grenville interval, this terminal collision is interpreted to be associated with the assembly of the supercontinent Rodinia, and in the Appalachian interval it is interpreted to be associated with the assembly of the supercontinent Pangea.

Even without considering other continents on Earth, the geological record of Paleoproterozoic collisional of Archean provinces combined with accretionary orogenesis at that time and through the rest of the Paleoproterozoic and Mesoproterozoic Eras provides strong evidence for mobile plate tectonics driving Laurentia's evolution throughout the past 2 billion years. This tectonic history inferred from geological data can be enhanced through integration with the paleomagnetic record.

#### 4.2 PALEOMAGNETIC POLE COMPILATION

In this chapter, I focus on the compilation of paleomagnetic poles developed through the Nordic Paleomagnetism Workshops with some additions and modifications (Fig. 3 and Table 2). The Nordic Paleomagnetism Workshops have taken the approach of using expert panels to assess paleomagnetic poles

and assign them grades meant to convey the confidence that the community has in these results (Evans et al., 2021). While many factors associated with paleomagnetic poles can be assessed quantitatively through Fisher statistics and the precision of geochronological constraints, other aspects such as the degree to which available field tests constrain the magnetization to be primary require expert assessment. The categorizations used by the expert panel are 'A' and 'B' with the last panel meeting occurring in Fall 2017 in Leirubakki, Iceland (Brown et al., 2018). The 'A' rating refers to poles that are judged to be of such high quality that they provide essential constraints that should be satisfied in paleogeographic reconstructions. The 'B' rating is associated with poles that are judged to likely provide a high-quality constraint, but have some deficiency such as remaining ambiguity in the demonstration of primary remanence or the quality/precision of available geochronologic constraints. Additional poles that were not given an 'A' or 'B' classification at the Nordic Workshops are referred to as not-rated ('NR'). These additional poles are taken from the Paleomagia database (Veikkolainen et al., 2014). Many of these poles in the Paleomagia database are quite valuable for reconstruction and should not be dismissed from being considered in paleogeographic reconstructions. However, there are ambiguities associated with many of the poles not given Nordic 'A' or 'B' ratings in terms of how well the nature of the remanence is constrained, including its age. For example, there are rich data associated with intrusive and metamorphic lithologies of the Grenville Province that are the available paleomagnetic constraints for Laurentia at the Mesoproterozoic–Neoproterozoic boundary. However, the ages of the remanence associated with these poles is complicated by the reality that the magnetization was acquired during exhumation and associated cooling within the Grenvillian orogen. Cooling ages of deeply exhumed lithologies are more difficult to robustly constrain than the ages of remanence associated with dated eruptive units or shallow-level intrusions. As a result, the vast majority of Grenville Province poles are not given an 'A' or 'B' rating with the exception of the 'B' rated pole from the ca. 1015 Ma Haliburton intrusions (Table 2). However, while any one of these Grenville poles could be interpreted to suffer from large temporal uncertainty, the overall preponderance of poles in a similar location at the time suggests that they need to be taken seriously within paleogeographic reconstructions of Laurentia (although an alternative view of an allochthonous origin put forward by Halls et al. (2015) is discussed below). In this compilation, the poles of Brown and McEnroe (2012) from the Adirondack highlands are used wherein the magnetic mineralogy and associated relative ages of remanence are relatively well-constrained (Table 2). An additional not-rated pole included in the present compilation is the new pole for the ca. 1144 Ma Ontario lamprophyre dikes (Piispa et al., 2018) that strengthens the position of Laurentia at the time and coincides with the position of the poles from the ca. 1140 Ma Abitibi dikes (Ernst and Buchan, 1993). This pole will likely receive an 'A' rating when assessed at the next Nordic paleomagnetism workshop. Poles from the Neoproterozoic Chuar Group of southwest Laurentia (ca. 760 Ma) as presented in Eyster et al. (2019) are also included.

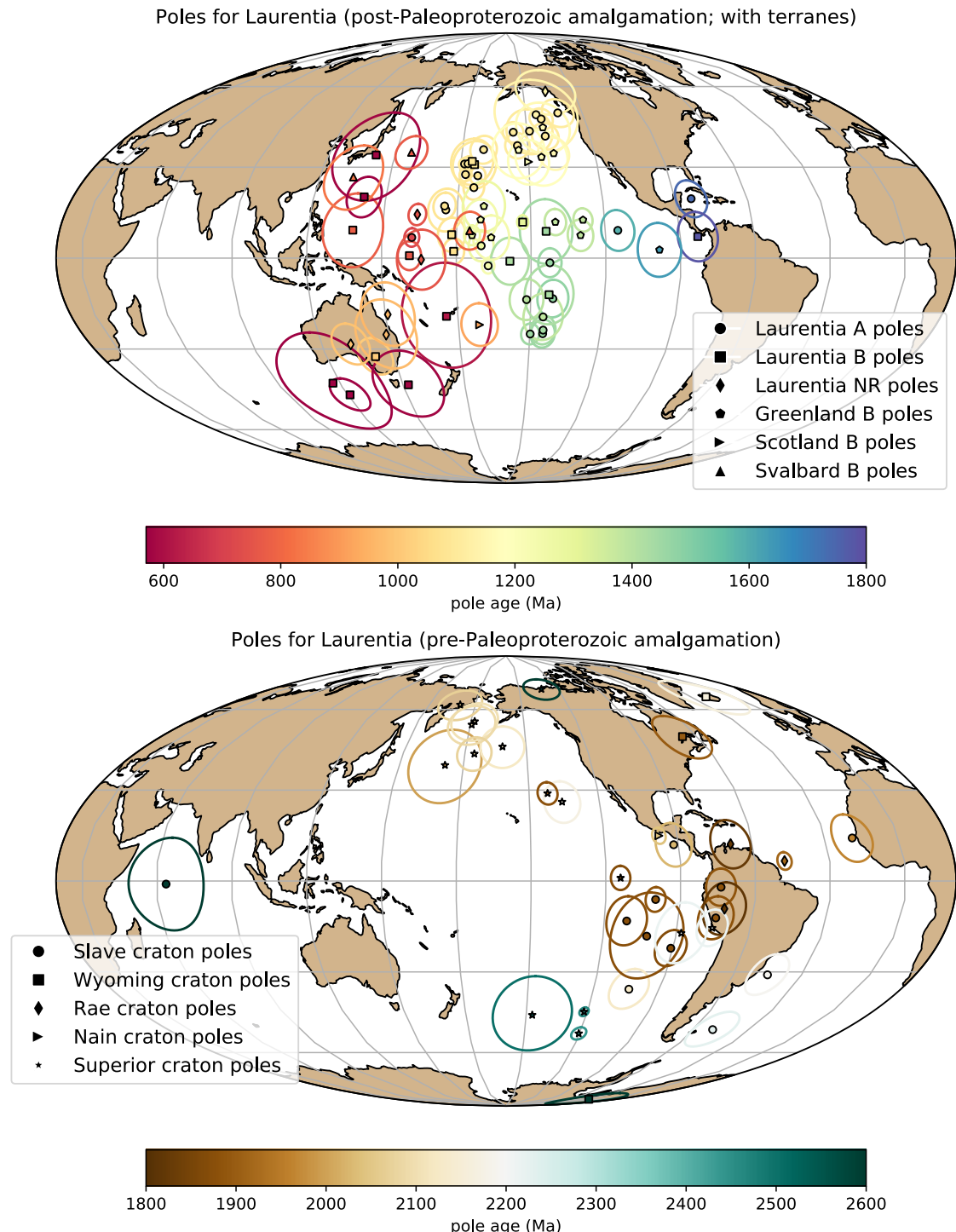


**Figure 3: Paleomagnetic poles from Laurentia.** Top panel: Paleomagnetic poles from 1800 to 560 Ma for Laurentia (including Greenland, Scotland and Svalbard). Bottom panel: Paleomagnetic data for Archean Provinces prior to the amalgamation of Laurentia.

#### 4.3 DIFFERENTIAL MOTION BEFORE LAURENTIA AMALGAMATION

Prior to the termination of the Trans-Hudson orogeny (before 1.8 Ga), paleomagnetic poles need to be considered with respect to the individual Archean provinces. For the Superior province, an additional complexity is that paleomagnetic poles from Siderian to Rhyacian Period (2.50 to 2.05 Ga) dike swarms, as well as deflection of dike trends, support an interpretation that there was substantial Paleoproterozoic rotation of the western Superior province relative to the eastern Superior province across the Kapuskasing Structural Zone (Bates and Halls, 1991; Evans and Halls, 2010). This interpretation is consistent with the hypothesis of Hoffman (1988) that the Kapuskasing Structural Zone represents major intracratonic uplift related to the Trans-Hudson orogeny. Evans and Halls (2010) propose an Euler rotation of (51°N, 85°W, -14°CCW) to reconstruct western Superior relative to eastern Superior and interpret that the rotation occurred in the time interval of 2.07 to 1.87 Ga. I follow this interpretation and group the poles into Superior (West) and Superior (East). Uncertainty remains with respect to whether the ca. 1.88 Ga Molson dikes pole pre-dates or post-dates this rotation (Evans and Halls, 2010) and thus for the time being should be considered solely in the western Superior province reference frame.

There are poles in the compilation for the Slave, Wyoming, Rae, Superior and North Atlantic provinces prior to Laurentia amalgamation (Fig. 3 and Table 2). Overall, these data provide an opportunity to re-evaluate the paleomagnetic evidence for relative motions between Archean provinces prior to Laurentia assembly. A lingering question raised in Hoffman (1988) is to what extent the Archean provinces each had independent drift histories with significant separation or shared histories before experiencing fragmentation and reamalgamation. The strongest analysis in this regard comes from comparisons between paleomagnetic poles between the Superior and Slave provinces (Buchan et al., 2009; Mitchell et al., 2014; Buchan et al., 2016). High-quality paleomagnetic poles from these two provinces provide strong support for differential motion between the Superior and Slave provinces between 2.2 and 1.8 Ga with the two provinces not being in their modern-day relative orientation to one another and having distinct pole paths as constrained by five time slices of nearly coeval poles from 2.23 and 1.89 Ga (Fig. 4; Buchan et al., 2016). These data provide paleomagnetic support for the Superior and Slave provinces having independent histories of differential motion. The data also support the hypothesis that the Trans-Hudson orogeny is the result of terminal collision associated with the closure of the Manikewan Ocean between the Superior province and the Hearne+Rae+Slave provinces. Reconstructions developed for this chapter of the Superior and Slave provinces using these poles are shown in Figure 4 and illustrate the difference in implied orientation and paleolatitude that results from these well-constrained poles.

#### 4.4 PALEOGEOGRAPHY OF AN ASSEMBLED LAURENTIA

Following the amalgamation of the Archean provinces in Laurentia ca. 1.8 Ga, poles from each part of Laurentia can be considered to reflect the position of the entire composite craton. It is worth considering the possibility that poles from zones of

Paleoproterozoic and Mesoproterozoic accretion could be allochthonous to the craton. Halls (2015) argued that this was the case for late Mesoproterozoic and early Neoproterozoic poles from east of the Grenvillian allochthon boundary fault. However, the majority of researchers have considered these poles to post-date major differential motion and be associated with cooling during collapse of a thick orogenic plateau developed during continent-continent collision (e.g. Brown and McEnroe, 2012). Poles with a B-rating are also included in the compilation that come from Greenland, Svalbard and Scotland. These terranes were once part of contiguous Laurentia, but have subsequently rifted away. These poles need to be rotated into the Laurentia reference frame prior to use for tectonic reconstruction, and I apply the rotations shown in Table 1. The Euler pole and rotation is quite well-constrained for Greenland as it is associated with recent opening of Baffin Bay and the Labrador Sea (for which the rotation of Roest and Srivastava, 1989 is used). The reconstruction of Scotland is associated with the opening of the Atlantic (for which the rotation employed by Torsvik and Cocks, 2017 is used) which is well-constrained, but has more uncertainty associated with the Euler pole than that for Greenland. The reconstruction of Svalbard is more challenging given a multi-stage tectonic history involving both translation within the Caledonides and subsequent rifting. The preferred Euler pole parameters of Maloof et al. (2006) are used here for this reconstruction. This Euler rotation is designed, in particular, to honor the high degree of similarity between Tonian sediments in East Greenland (Hoffman et al., 2012) and those of East Svalbard (Maloof et al., 2006) and to reconstruct East Svalbard to be aligned with these correlative sedimentary rocks.

Table 1: Rotations of separated terranes

Block	Euler pole longitude	Euler pole latitude	rotation angle	note and citation
Greenland	-118.5	67.5	-13.8	Cenozoic separation of Greenland from Laurentia associated with opening of Baffin Bay and the Labrador Sea (Roest and Srivastava, 1989)
Scotland	161.9	78.6	-31.0	Reconstructing Atlantic opening following Torsvik and Cocks (2017)
Svalbard	125.0	-81.0	68	Rotate Svalbard to Laurentia in fit that works well with East Greenland basin according to Maloof et al. (2006)

Through the Proterozoic, there are intervals where there are abundant paleomagnetic poles that constrain Laurentia's position and intervals when the record is sparse (shown colored by age in Fig. 3). To further visualize the temporal coverage of the poles and to summarize the motion, implied paleolatitudes for an interior point on Laurentia are shown in Figure 5. The ages of the utilized paleomagnetic poles are also shown in comparison to the simplified summary of tectonic events in Figure 2. Both collisional and extensional tectonism can result in the formation of lithologies that can be used to develop paleomagnetic poles either as a result of basin formation, magmatism or both. In addition, intraplate magmatism resulting from plume-related large-igneous provinces (LIPs) can lead to paleomagnetic poles in periods that are otherwise characterized by tectonic quiescence (e.g. the ca. 1267 Ma Mackenzie LIP; Fig. 2). Intra-

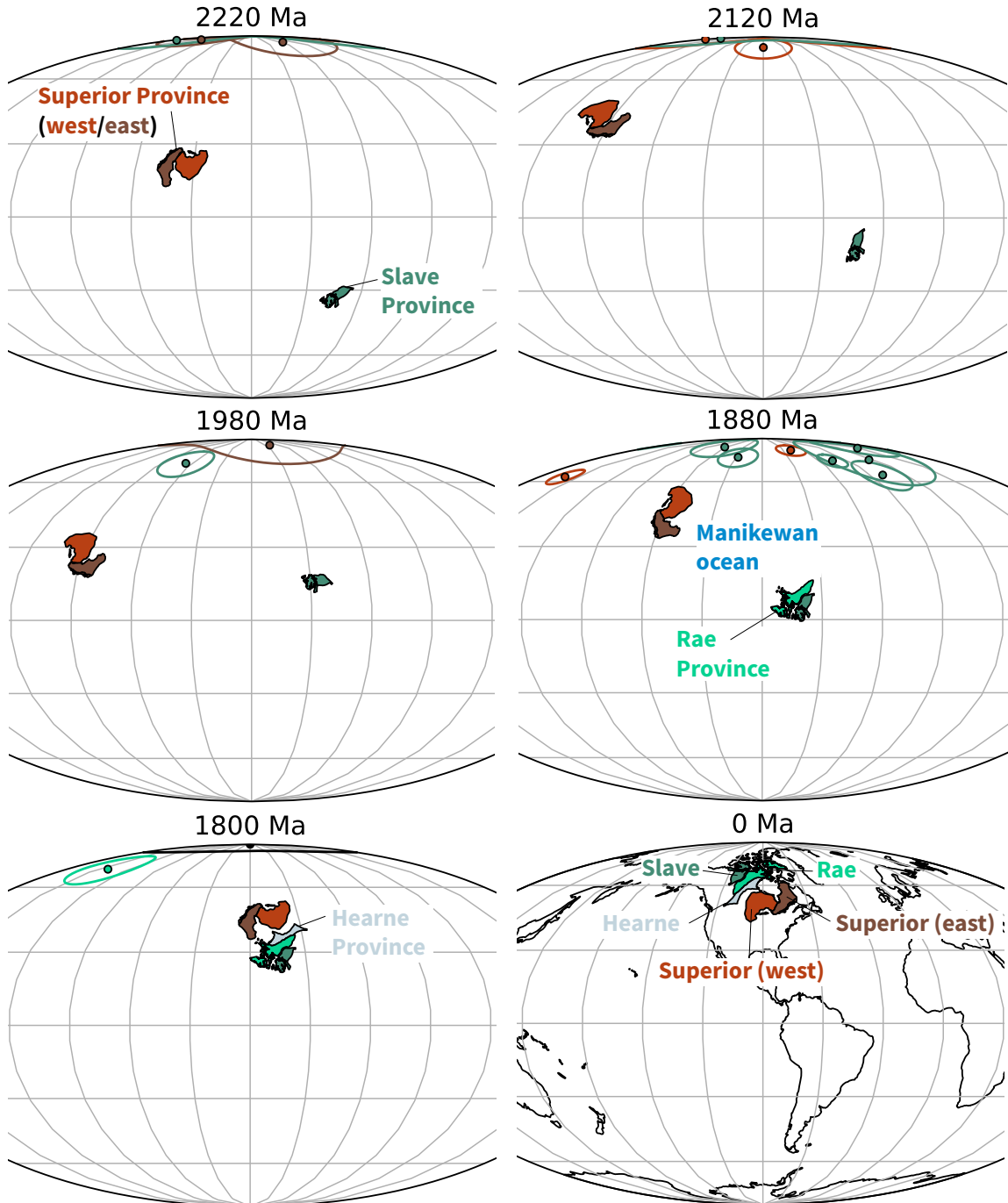


**Figure 4: Paleogeographic reconstructions developed using poles from the Superior, Slave and Rae provinces.** The polarity options that are chosen for the provinces are those that minimize total apparent polar wander path length. This model reconstructs a wide Manikewan ocean that underwent orthogonal closure rather than an alternative possibility of narrower Manikewan with a pivot-like closure. Paleomagnetic poles are shown colored to match their respective province with these provinces shown in present-day coordinates and labeled in the 0 Ma panel. Poles with ages that are within 25 million years of the given time slice are shown. The relatively well-resolved pole paths from the Superior and Slave provinces (Fig. 3) that are utilized for these reconstructions provide strong support for differential plate tectonic motion between 2220 and 1850 Ma.

continental rifts have led to the highest density of poles both in the case of the ca. 1.4 Ga Belt Supergroup and the ca. 1.1 Ga Midcontinent Rift (Fig. 2). The quality and resolution of the record from the Midcontinent Rift is aided by the voluminous magmatism that occurred in conjunction with basin formation that enables the development of a well-calibrated apparent polar wander path (Swanson-Hysell et al., 2019). The late Tonian Period also has a number of poles including the Gunbarrel LIP (ca. 780 Ma) and Franklin LIP (ca. 720 Ma), as well as similarly-aged sedimentary rocks from western Laurentia basins (Eyster et al., 2019). Overall, there is internal consistency among the paleomagnetic poles within intervals for which there is high-resolution coverage. These data result in progressive paths such as ascending up to the Logan Loop, down the Keweenawan Track (Swanson-Hysell et al., 2019) to the Grenville Loop prior to a temporal gap before the late Tonian (ca. 775 to 720 Ma) path (Eyster et al., 2019).

Data from other terranes add resolution to the record. In particular, data from Greenland add 12 poles between 1385 and 1160 Ma when there are only four poles from mainland Laurentia. Given that the rotation between Greenland and mainland Laurentia is well-constrained (Table 1), once rotated these poles can be used for reconstruction of the entire continent. The reliability of this approach gains credence through the good agreement between the ca. 1633 Ma Melville Bugt diabase dikes pole from Greenland (Halls et al., 2011) and the ca. 1590 Ma Western Channel diabase pole of mainland Laurentia (Irving and Park, 1972; Figs. 3 and 5). Similarly, there is good agreement between the ca. 1267 Ma Mackenzie dikes pole of Laurentia (Buchan et al., 2000) and coeval poles from Greenland such as the ca. 1275 Ma North Qoroq intrusives (Piper, 1992) and Kungnat Ring dike (Piper, 1977). Furthermore, the Greenland poles with ages that fall between the ca. 1237 Ma Sudbury dikes and ca. 1144 Ma lamprophyre dikes pole of mainland Laurentia are consistent with constraints on either side from the mainland while filling in the ascending limb of the path leading up to the apex of 1140 to 1108 Ma poles known as the Logan Loop (Figs. 3 and 5).

An exception to this overall agreement between poles from Greenland and mainland Laurentia occurs ca. 1382 Ma. There are poles of this age from Greenland associated with the Zig-Zag Dal basalts and related intrusions (Marcussen and Abrahamsen, 1983; Abrahamsen and Van Der Voo, 1987). However, these poles are in a distinct location from poles of similar age associated with the Belt Supergroup (e.g. the McNamara Formation and Pilcher/Garnet Range and Libby Formations; Elston et al., 2002). Additionally, the older Belt Supergroup poles form a more southerly population than time-equivalent poles from elsewhere in Laurentia such as the Mistastin Pluton. There are potential complications associated with the Belt Supergroup being exposed within thrust sheets with significant Cenozoic Mesozoic and Cenozoic deformation. However, vertical axis rotations of the Belt region are not able to bring the Belt poles into agreement with those from Laurentia or Greenland nor is translation away from the craton. Another potential complication is that the remanence used for the development of the Belt Supergroup resides in hematite. As a result, there is the potential for inclination-flattening within the sedimentary rocks from which poles are developed. However, applying a moderate inclination factor of  $f = 0.6$  also does not bring the poles

into congruence with the Zig-Zag basalts. There is the potential that the hematite could be the result of post-depositional oxidation (the remanence of the lavas pole is also held by hematite), however the overall coherency of the pole directions and the presence of reversals as interpreted from antipodal directions has been taken as evidence that the remanence is primary (Elston et al., 2002). At present, it is unclear which poles are a better representation of Laurentia's position ca. 1400 Ma.

Another challenging portion of the Laurentia paleomagnetic record is that for the Ediacaran Period at the end of the Neoproterozoic era where there are inconsistencies between poles of similar age (Figs. 3 and 5). As a result, there are poles that imply both low-latitude and high-latitude positions of Laurentia between 583 and 565 Ma (Fig. 5). This conflicting record is a longstanding problem and has led to the presentation of both high-latitude and low-latitude Laurentia paleogeographic reconstructions at the time (e.g. Pisarevsky et al., 2001; Li et al., 2008). One explanation for these variable pole positions is that they are the result of large-scale oscillatory true polar wander in the Ediacaran where rapid rotation of the entire silicate Earth influenced poles in Baltica and West Africa as well (McCausland et al., 2007; Robert et al., 2017). Paleodirectional data from single feldspar crystals from the Sept-Îles layered intrusion led Bono and Tarduno (2015) to interpret the lower inclination (and therefore lower latitude) direction from the intrusion (the one included as the ca. 565 Ma Sept-Îles pole in Table 2; Tanczyk et al., 1987) as the primary thermal remanent magnetization. Bono and Tarduno (2015) interpret steeper directions also recovered from the intrusives as the result of remagnetization. They suggest that other steep magnetizations from Ediacaran Laurentia plutonic rocks, such as that observed in the ca. 583 Ma Baie des Mountons complex (the A group of McCausland et al. (2011) in Table 2), are also the result of remagnetization. Notably the lower inclination Baie des Mountons complex B Group directions result in a pole that is indistinguishable from the lower inclination Sept-Îles intrusives pole. Another possibility discussed in the literature is that the lack of congruency between poles in this time interval is due to a particularly weak and non-dipolar geomagnetic field (Abrajevitch and Van der Voo, 2010; Halls et al., 2015; Bono et al., 2019). Data from the ca. 585 Ma Grenville dyke swarm of Laurentia interpreted as primary reveal  $\sim 90^\circ$  differences in direction within dikes dated within to  $2.5 \pm 0.9$  million years of one another (Halls et al., 2015). The rates of  $>26^\circ/\text{Myr}$  ( $>288 \text{ cm/yr}$ ) implied if these data are interpreted as resulting from plate motion or true polar wander were considered as dynamically implausible by Halls et al. (2015) leading the authors to favor a deviation from axial dipolar behavior as the explanation for disparate Ediacaran directions. Estimates of magnetic paleointensity in these Grenville dikes are anomalously weak which could support a deviation from stable axial dipolar geomagnetic field behavior at the time (Thallner et al., 2020). Regardless of mechanism, the Ediacaran data stand out as anomalous relative to the coherency of the rest of the poles in the compiled record for Laurentia (Fig. 5).

Synthesizing the compilation of paleomagnetic poles for Laurentia into a composite path over the past 1.8 billion years presents a challenge given the highly variable temporal coverage. The method typically applied in the Phanerozoic is to develop synthesized pole paths either through fitting spherical

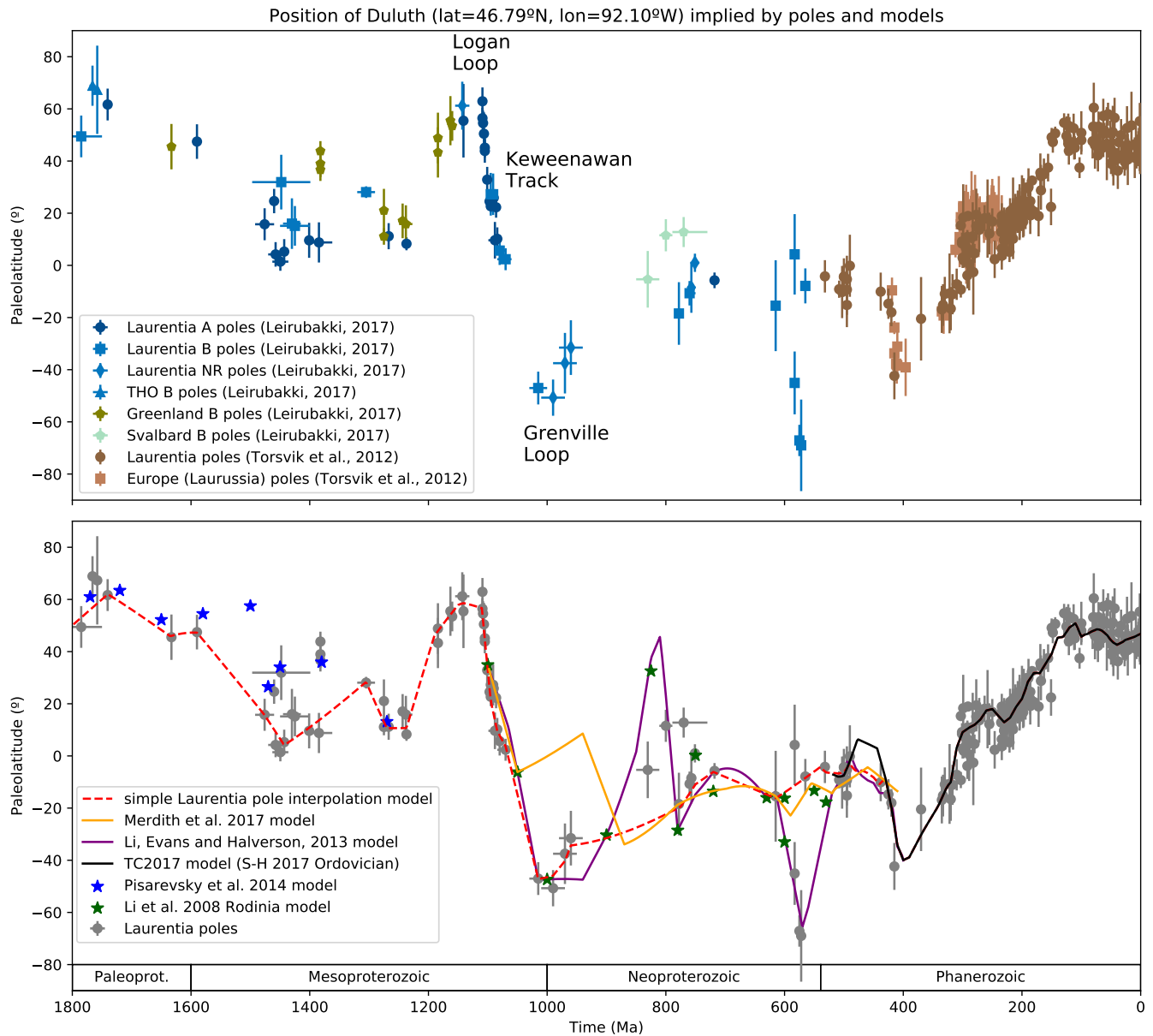


**Figure 5: Laurentia paleolatitude through time in data and models.** Top panel: Paleolatitude implied by paleomagnetic poles from Laurentia and associated blocks for Duluth ( $\text{lat}=46.79^{\circ}\text{N}$ ,  $\text{lon}=92.10^{\circ}\text{W}$ ). The paleomagnetic poles are compiled in Table 2. Bottom panel: Paleolatitude implied by Laurentia poles compared with that implied by published paleogeographic models and the simple Laurentia model used in this chapter for the reconstructions in Figure 6.

splines through the data or calculating binned running means where the Fisher mean of poles within a given interval are calculated (Torsvik et al., 2012). Applying such an approach can reduce the influence of spurious poles. Such synthesis is particularly important in regions of high data density where seeking to satisfy every mean pole position would result in jerky motion.

A synthesized pole path for Laurentia is developed here and used to develop a paleogeographic reconstruction of Laurentia constrained by the compilation of paleomagnetic poles. The paleolatitude implied by this continuous model is shown in Figure 5. This path is based on Laurentia data alone which means that it is poorly constrained through intervals of sparse data (950–850 Ma for example). One could use interpretations of paleogeographic connections with other cratons (e.g. Baltica in the early Neoproterozoic) to fill in such portions of the path, however the result then becomes model-dependent without being constrained by data from Laurentia itself. In portions of the record with a more dense record of poles, such as ca. 1450 Ma, a calculated running mean is used to integrate constraints from multiple poles. This method follows the approach taken in the Phanerozoic (e.g. Torsvik et al., 2012 wherein all poles within a 20 Myr interval are averaged with the interval than progressively moved forward in 10 Myr steps. When there are isolated ‘A’ grade poles without other temporally-similar poles, these poles are fully satisfied in model. Where there are no constraints a simple interpolation between constraints is made. While data from Scotland and Svalbard are associated with Laurentia, the Scotland poles are poorly constrained in time and the Svalbard rotation to Laurentia is uncertain. These poles are not utilized in the simple Laurentia model which means that the model as shown does not include oscillatory true polar wander interpreted to have occurred ca. 810 and 790 Ma based on data from Svalbard (Maloof et al., 2006). The model of Li et al. (2013) shown in Figure 5 does seek to incorporate this true polar wander while also incorporating an interpretation of the paleomagnetic pole record from South China (albeit one that needs to be revisited given updates to the paleomagnetic and geochronologic record from South China; Zhang et al., 2021).

One downside of a running mean approach is that it pulls the mean to regions of high data density. As was shown in Swanson-Hysell et al. (2019), this behavior can reduce motion along an apparent polar wander path. As a result, for the portion of the reconstruction during the interval of time ca. 1110 to 1070 Ma where there is high data density from the Midcontinent Rift, I utilize an Euler pole inversion from Swanson-Hysell et al. (2019).

Paleogeographic snapshots for the past position of Laurentia reconstructed using this synthesis of the paleomagnetic poles are shown in Figure 6. These reconstructions use the tectonic elements as defined by Whitmeyer and Karlstrom (2007) with these elements being progressively added associated with Laurentia’s accretionary growth. As a reminder to the reader, paleomagnetic poles provide constraints on the paleolatitude of a continental block as well as its orientation (which way was north relative to the block). While they provide constraints in this regard, they do not provide constraints in and of themselves for the longitudinal position of the block. Other approaches to obtain paleolongitude utilize geophysical hypothe-

ses such as assuming that large low shear velocity provinces have been stable plume-generating zones in the lower mantle to which plumes can be reconstructed (Torsvik et al., 2014) or that significant pole motion in certain time intervals is associated with true polar wander axes with specified paleolongitudes that switch through time in conjunction with the supercontinent cycle (Mitchell et al., 2012). In Figure 6, the map projections are centered on the longitudinal position of Duluth with the orientation and paleolatitude being constrained by the paleomagnetic pole compilation as synthesized in the simple Laurentia pole interpolation model (Fig. 5).

#### 4.5 COMPARING PALEOGEOGRAPHIC MODELS TO THE PALEOMAGNETIC COMPILATION

Developing comprehensive global continuous paleogeographic models is a major challenge given the need to integrate and satisfy diverse geological and paleomagnetic data types. Continually improving constraints related to tectonic setting from improved geologic and geochronologic data need to be carefully integrated with the database of paleomagnetic poles. Paleomagnetic pole compilations themselves are evolving with better data and improved geochronology (Evans et al., 2021). Efforts such as this volume are therefore essential to present the state-of-the-art in terms of existing constraints that can be used to evaluate current models and set the stage for future progress in Precambrian paleogeography.

There is an overall lack of models in the literature for the Proterozoic with published continuous rotation parameters that can be compared to the compilation of paleomagnetic poles presented herein. The approach in the community for many years has been to publish models as snapshots at given time intervals presented in figures without publishing continuous rotation parameters, although some studies have published the Euler rotations associated with specified times. With the further adoption of software tools such as GPlates, there has been significant progress in the publication of continuous paleogeographic models constrained by paleomagnetic poles through the Phanerozoic (540 Ma to present; e.g. Torsvik and Cocks, 2017).

An exception to the paucity of published continuous paleogeographic models for the Precambrian is the Neoproterozoic model of Merdith et al. (2017) which is shown in comparison to the constraints for Laurentia in Figure 5. The extent to which the implied position of Laurentia in Merdith et al. (2017) is consistent with the compiled paleomagnetic constraints can be visualized in Figure 5. As noted above, the development of such models is challenging and the researchers need to balance varying constraints. The focus here will be on the extent to which this model satisfies the available paleomagnetic poles for Laurentia. The model does not honor the Grenville loop (e.g. Laurentia going to moderately high southerly latitudes ca. 1000 Ma), which is a striking departure from the paleomagnetic record and standard paleogeographic models. Additionally, the implemented plate motion strays from the younger poles of the Keweenawan Track and does not honor the Franklin LIP pole Denyszyn et al. (2009b) despite its ‘A’ Nordic rating. The Franklin pole is taken to be a key constraint at the Tonian/Cryogenian boundary that provides evidence both for the supercontinent Rodinia being equatorial and for ice sheets

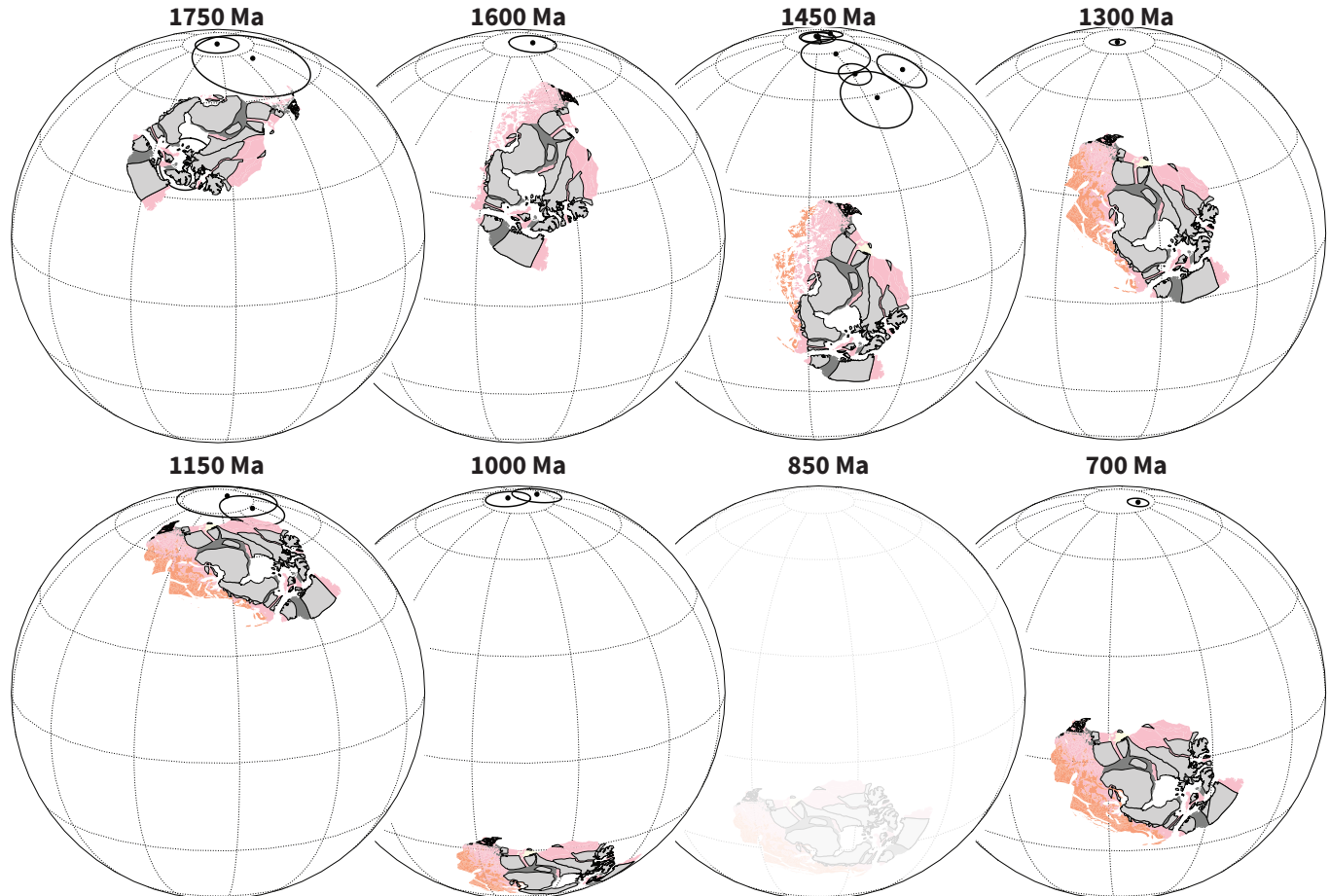


**Figure 6: Paleogeographic reconstructions of Laurentia at time intervals through the Proterozoic that are well-constrained by paleomagnetic data.** These reconstructions use the simple Laurentia pole interpolation model that is shown in Figure 5 and use this model to reconstruct the tectonic elements of Whitmeyer and Karlstrom (2007) shown in Figure 1. Modern coastlines are maintained in these polygons so that the rotated orientations can be interpreted by the reader in comparison to Figure 1. Paleomagnetic poles within 25 million years of each reconstruction time are plotted. All reconstructions have poles within such a time frame that provide constraints with the exception of the 850 Ma reconstruction which is shown faintly given this relative uncertainty in Laurentia's position.

associated with the Sturtian glaciation having extended to equatorial latitudes (Macdonald et al., 2010).

There are more published models that show snapshots and publish rotation parameters associated with given time intervals such as the Rodinia model of Li et al. (2008) and the Mesoproterozoic model of Pisarevsky et al. (2014), without providing parameters for a continuous model. The position for Laurentia implied by the Euler poles given for the model snapshots of these studies are shown in Figure 5 and can be compared to the compiled record. The figure also shows the continuous implied position of Laurentia from the late Mesoproterozoic into the early Paleozoic from the model of (Li et al., 2013; while the model parameters were not published with that study they have now been made available by the authors).

#### 4.6 PALEOENVIRONMENTAL CONSTRAINTS ON PALEOLATITUDE

Sedimentary rocks whose deposition is associated with specific climatic conditions have the potential to provide insight into paleolatitude. Relevant deposits in the Proterozoic include glacial deposits deposited by continental ice sheets, carbonates deposited in carbonate-saturated (and thereby likely to be warm) marine environments, and evaporite deposits deposited where evaporation exceeded precipitation. Interpretations of paleolatitude based on glacial deposits are complicated by the evidence for multiple global and low-latitude glacial intervals during the Proterozoic (Evans, 2003). Evaporite deposits are particularly compelling as paleolatitude constraints given that their deposition is interpreted to be associated with arid regions resulting from large-scale Hadley cell downwelling (Evans, 2006). While moisture in the subtropics can change along with Earth's climate, the overall pattern of  $\sim 10\text{--}35^\circ$  of latitude being where annual mean evaporation exceeds precipitation persists (Burls and Fedorov, 2017). Using a compilation of paired paleomagnetically-determined paleolatitude constraints and evaporite occurrence, Evans (2006) demonstrated that over the past 2 billion years large-scale evaporite deposition was consistently located in subtropical latitudes that correspond to the latitudes of modern arid zones. This finding is consistent both with the geocentric axial dipole hypothesis used to calculate paleolatitude and the long-term stability of large-scale convection circulation cells.

There is high evaporation in the subtropics and tropics. Within the tropical rain belt (0 to  $\sim 10^\circ$  latitude) these high evaporation rates are typically overwhelmed by precipitation such that global zonal mean precipitation exceeds evaporation within  $\sim 10^\circ$  of the equator (within  $\sim 8^\circ$  of the equator over land) with evaporation exceeding precipitation from those latitudes towards higher ones with evaporation minus precipitation being at a maximum at  $\sim 20\text{--}25^\circ$  (Park et al., 2020). However, continental interiors near the equator can also be arid due to regional precipitation patterns leading to the precipitation of evaporites. For example, Lake Magadi in Kenya at a latitude of  $1.9^\circ$  S is a saline lake where thick bedded evaporites have accumulated (Eugster, 1980). Caution is therefore needed when interpreting paleolatitude from evaporites in terrestrial and intracratonic settings given that they could occur both in tropical and subtropical latitudes.

Proterozoic evaporite deposits are documented within these units that were deposited following the amalgamation of Laurentia:

- The Altyn Formation of the Belt Supergroup contains pseudomorphs after gypsum crystals and anhydrite within shallow-water carbonates with relict gypsum and anhydrite preserved within secondary silica (White, 1984). The correlative Prichard Formation is intruded by  $1468.8 \pm 2.5$  Ma sills (Sears et al., 1998). Halite molds and casts are present within mudstones of the overlying Grinell Formation (Pratt and Ponce, 2019). Higher in the Belt Supergroup stratigraphy, within the Wallace Formation, there is stratiform scapolite — a metamorphic mineral interpreted to have formed from a halite precursor within the Wallace Formation (Hietanen, 1967). There are also halite and gypsum pseudomorphs within carbonate mudstones of the correlative to underlying Helena Formation (Pratt, 2001; Winston, 2007). These deposits are older than the  $1443 \pm 7$  Ma Purcell lavas and further constrained in age by a tuff with a U-Pb date of  $1454 \pm 9$  Ma within the Helena Formation (Evans et al., 2000).
- The Mesoproterozoic Iqqittuq Formation of the Borden basin (formerly part of the Society Cliffs Formation) contains bedded gypsum deposits (massive and laminated with beds that reach a thickness of 2.5 meters) and shale with halite casts (Kah et al., 2001). These deposits are bracketed between Re-Os dates of  $1048 \pm 12$  Ma for an underlying shale and  $1046 \pm 16$  Ma for an overlying shale (Gibson et al., 2018).
- The Tonian Ten Stone Formation of the Mackenzie Mountains Supergroup (formerly known as the Gypsum Formation) contains a  $\sim 500$  meter thick succession dominated by gypsum with minor anhydrite interpreted to have been deposited in a deep-water (below wave base) restricted marine basin (Turner and Bekker, 2016). These thick bedded sulfate deposits are older than cross-cutting  $777.7 \pm 2.5$  Ma sills of the Gunbarrel large igneous province (U-Pb date from Jefferson and Parrish, 1989) and younger than ca. 1005 Ma detrital zircons (Turner and Bekker, 2016). The overlying Ram Head Formation has been correlated with the Bitter Springs Stage which is constrained between  $811.5 \pm 0.3$  Ma and  $788.7 \pm 0.2$  Ma (Macdonald et al., 2010; Swanson-Hysell et al., 2015) suggesting that the evaporites are ca. 820 Ma (Turner and Bekker, 2016). These deposits are hypothesized to be correlative with sulfate evaporites within the Minto Inlet Formation of the Shaler Supergroup (Jones et al., 2010; Turner and Bekker, 2016).
- The Tonian Kilian Formation of the Shaler Supergroup contains nodules of gypsum and anhydrite interpreted to have been deposited in an intertidal to supratidal evaporitic mudflat environment (Prince, 2014). The Kilian Formation is interpreted to post-date the Bitter Springs Stage and be correlative with the Redstone River Formation of the Coates Lake Group in the McKenzie Mountains that contains bedded gyp-

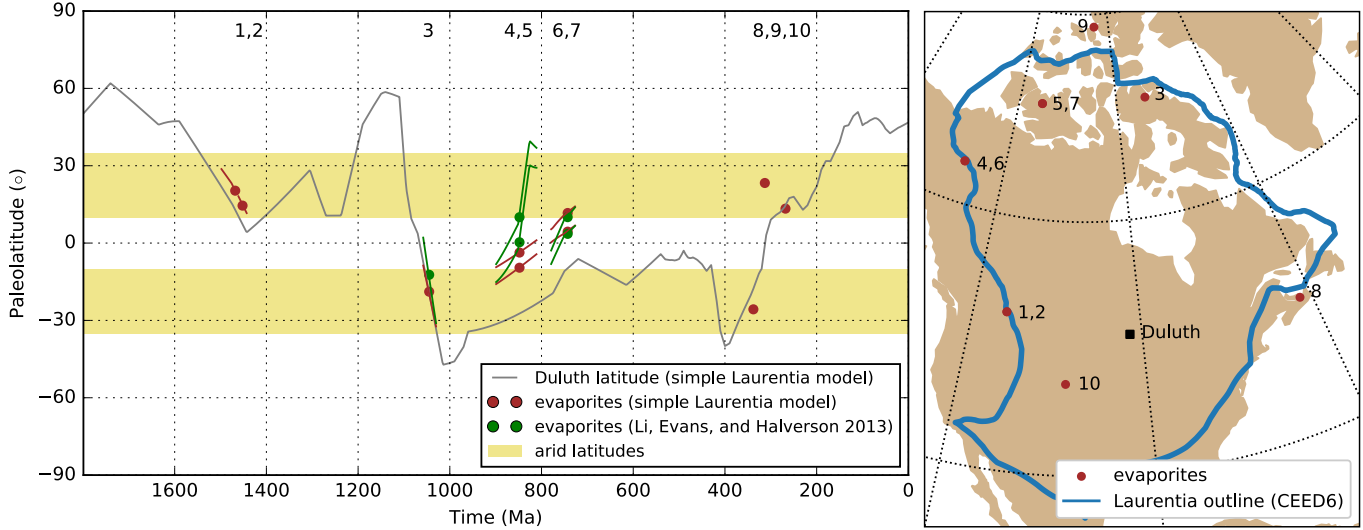


**Figure 7: Paleolatitude of Laurentia evaporites.** Left panel: The paleolatitude of evaporite deposits following the amalgamation of Laurentia as reconstructed by the simple Laurentia model shown in Fig. 5 combined with the Phanerozoic model of Torsvik and Cocks (2017) and as reconstructed by the model of Li et al. (2013) for the Neoproterozoic. Proterozoic evaporite deposits in this panel are discussed in the text while Phanerozoic ones are taken from the compilation of Evans (2006). The evaporite lines extend from the maximum to minimum age constraints while the points are at the preferred depositional age. Right panel: The present-day location of evaporites reconstructed to the left. 1: Altyn Formation (Belt Supergroup), 2: Wallace/Helena Formations (Belt Supergroup), 3: Iqqittuq Formation (Bylot Supergroup), 4: Ten Stone Formation (Mackenzie Mountains Supergroup), 5: Minto Inlet Formation (Shaler Supergroup), 6: Redstone River Formation (Mackenzie Mountains Supergroup), 7: Kilian Formation (Shaler Supergroup), 8: Carboniferous Canadian Maritime, 9: Carboniferous Sverdrup, 10: Permian Midcontinental USA.

sum as well as gypsum-bearing siltstone (Jefferson and Parrish, 1989; Jones et al., 2010). The Redstone River Formation is younger than the  $777.7 \pm 2.5$  Ma volcanics and older than a  $732.2 \pm 4.7$  Ma Re-Os isochron from the overlying Coppercap Formation (?).

In Figure 7, the paleolatitude of these evaporite deposits are reconstructed using the simple Laurentia model developed in this work as well as with the Li et al. (2013) model for the late Mesoproterozoic to Neoproterozoic. The position of major Phanerozoic evaporite basins of North America are also shown with their paleolatitude reconstructed with the paleogeographic mode of Torsvik and Cocks (2017). These paleogeographic models reconstruct evaporite deposition to have been within  $30^\circ$  of the equator in both the Phanerozoic and Proterozoic. In the Tonian period, evaporite deposition may have occurred equatorward of  $10^\circ$  (Fig. 7 which may reflect increased aridity in the tropical interior of the Rodinia supercontinent.

#### 4.7 EVALUATING LAURENTIA'S PROTEROZOIC PALEOGEOGRAPHIC NEIGHBORS

Many different paleogeographic connections between Laurentia and other Proterozoic cratons that have been proposed and utilized in paleogeographic models both prior to and following the amalgamation of Laurentia's constituent Archean provinces to form Laurentia. This section does not seek to be comprehensive in this regard, but rather I seek to highlight and contextualize some of the more prominent and/or well-supported models.

Note that this section is currently under development and is incomplete

##### 4.7.1 Amazonia

In the central and southern Appalachians there are inliers of rocks that were metamorphosed during the Ottawan phase of the Grenvillian orogeny (McLelland et al., 2013). On the basis of whole-rock Pb-isotope data, Loewy et al. (2003) and Fisher et al. (2010) proposed that these inliers are fragments of Amazonia lithosphere that were transferred to Laurentia during the orogeny and left behind when the Iapetus Ocean formed. In particular, Fisher et al. (2010) suggest the Sunsás orogen of Amazonia as the best match for southern and central Appalachian inliers. This positioning leads to a paleogeographic model wherein Amazonia is a major portion of the conjugate continental lithosphere that collided with Laurentia during Rodinia assembly (Evans, 2013; Cawood and Pisarevsky, 2017). While the lack of ca. 1100 and ca. 1000 Ma poles from Amazonia precludes a robust paleomagnetic test, this scenario is consistent with the available late Mesoproterozoic poles from Amazonia (ca. 1200 Nova Floresta pole and ca. 1150 Fortuna Formation pole; D'Aarella-Filho et al., this volume) as shown in Evans et al. (2013). In this paleogeographic scenario, the basement inliers of the Appalachian Orogen in the Blue Ridge region are interpreted to be the leading edge of Amazonia with initial collision ca. 1080 Ma initiating the Ottawan phase of the Grenvillian orogeny (Fig. 2). Subsequent separation of Amazonia would have led to the formation of the Iapetus Ocean as Rodinia rifted apart. Departure of Amazonia potentially oc-

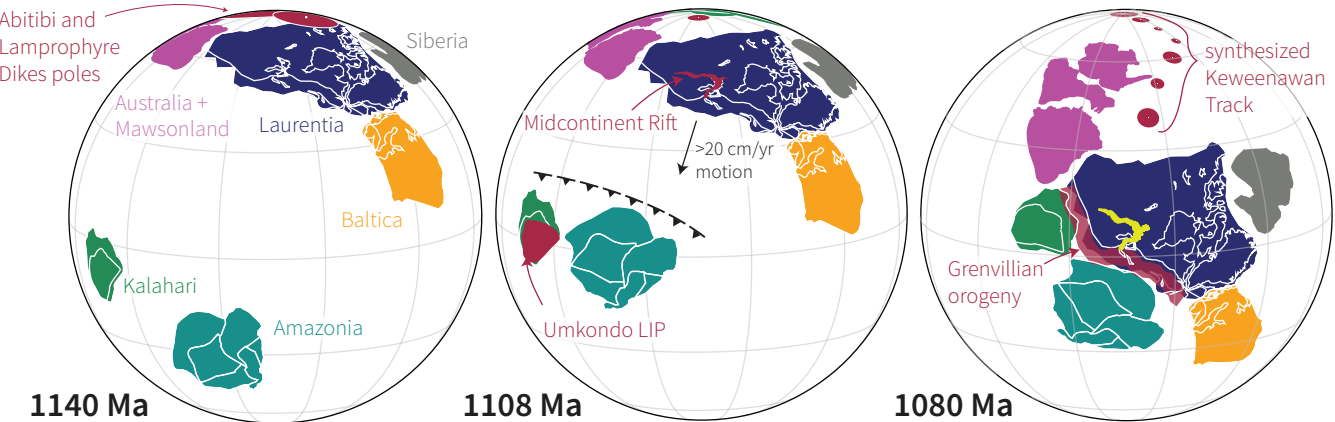


**Figure 8: Paleogeographic reconstructions of Laurentia and other select Proterozoic continents leading up to Rodinia assembly in the late Mesoproterozoic.** This reconstruction is modified from Swanson-Hysell et al. (2019). The record of paleomagnetic poles implies rapid motion which is consistent with the timing of collisional orogenesis associated with the Grenvillian orogeny.

curred as early as ca. 700 Ma in the Paleo-Iapetus Ocean model of Robert et al. (2020).

#### 4.7.2 Australia

#### 4.7.3 Baltica

Based on correlation of Archean provinces and Paleoproterozoic orogenic belts, Gower et al. (1990) reconstructed Baltica to Laurentia in a position known as the NENA (northern Europe and North America) configuration. This connection proposes a tight fit between modern-day northern Norway and Russia's Kola Peninsula with eastern Greenland (Gower et al., 1990, Salminen et al., this volume). In this position, Baltica and Laurentia are hypothesized to share a long-lived accretionary margin (Karlstrom et al., 2001). This reconstruction is brings paleomagnetic poles

compatible with existing paleomagnetic constraints from ca. 1750 to 1270 Ma Evans and Pisarevsky (2008) and these conjoined cratons feature as a major component of the hypothesized Nuna supercontinent (Evans and Mitchell, 2011; Zhang et al., 2012; .

#### 4.7.4 Kalahari

High-quality paleomagnetic poles constrain the coeval Umkondo large igneous province of the Kalahari craton and the early flood basalts of the Midcontinent Rift of Laurentia to have been separated by more than  $50^{\circ}$  of latitude at the time they were emplaced with the craton margins separated by more than  $30^{\circ}$  of latitude (Swanson-Hysell et al., 2015). These data make it difficult to envision a shared origin of magmatism and pose a challenge to approaches that seek to reconstruct paleogeography on the basis on ages of LIPs alone. However, with the subsequent rapid motion of Laurentia to low latitudes it is possible that the Kalahari was a conjugate craton to the (south)east margin of Laurentia during the time of the Grenvillian orogeny. This conjugate relationship based on the interpretation that the Namaqua-Natal belt in southern

Kalahari records late Mesoproterozoic collisional orogenesis was proposed in Hoffman (1991) and is implemented in many reconstructions of Rodinia (e.g. Li et al., 2008). Whether the Grenvillian margin of Laurentia and the Namaqua-Natal belt of Kalahari faced one another and been conjugates can be evaluated by paired paleomagnetic and geochronologic data sets from the Umkondo LIP and the Midcontinent Rift. The preferred interpretation of Swanson-Hysell et al. (2015) and (Kasbohm et al., 2015) was that sites with northerly declinations from the Umkondo Province correspond to the reversed polarity directions from the early magmatic stage in the Midcontinent Rift (e.g. Swanson-Hysell et al., 2014a) such that Namaqua-Natal margin faced the Grenvillian margin of Laurentia. The late Mesoproterozoic apparent polar wander paths for Laurentia and Kalahari are consistent with them become conjoined as in Figure 8 (Swanson-Hysell et al., 2015). The record of the Namaqua belt wherein there is granitoid plutonism and arc accretion up to ca. 1090 followed by peak granulite metamorphism ca. 1065 to 1045 Ma (Diener et al., 2013; Spencer et al., 2015) is consistent with a scenario wherein Kalahari was on the upper plate that collided with Laurentia at the time of the Ottawa phase of Grenvillian orogenesis following subduction of oceanic lithosphere associated with an intervening ocean. If they indeed became conjoined in Rodinia, the separation of Kalahari from Laurentia likely initiated ca. 795 Ma heralded by the emplacement of the Gannakouriep diabase dike swarm (Rioux et al., 2010; de Kock et al., 2021).

#### 4.7.5 North China

The latest Mesoproterozoic to earliest Neoproterozoic pole path of the North China craton includes a swath of paleomagnetic poles with a similar arc length to the Keweenawan Track to Grenville Loop of Laurentia's APWP (Zhao et al., 2019; Zhang et al., this volume). While the chronostratigraphic age constraints on these North China poles are much looser than those from Laurentia, Zhao et al. (2019) propose that the North China poles can be aligned with the Keweenawan Track to reconstruct

North China as being conjoined to the northwest margin of Laurentia from prior to ca. 1110 Ma into the early Neoproterozoic. North China would have been at polar latitudes ca. 1110 Ma and moved rapidly with Laurentia as it transited towards the equator. Zhao et al. (2019) also argued that similarity in the detrital zircon age spectra between early Neoproterozoic sediments in NW Laurentia and North China basins supports this reconstruction. In particular, sediment transport from Laurentia could provide a source for ca. 1.18 Ga zircons (from the Shawinigan orogen) and ca. 1.08 Ga zircons (from the Grenville orogen). In the Laurentia basins, ca. 1.6 Ga zircons without a clear Laurentia source could be sourced from North China craton granites (e.g. Wang et al., 2020). If North China was in this position, the timing of its arrival adjacent to Laurentia is unclear. The ca. 1220 Ma dikes pole of the North China craton is not coincident with the ca. 1237 Ma Sudbury dikes pole in this reconstructed position leading Zhao et al. (2019) and Zhang et al. (this volume) to suggest that North China arrived on the Laurentian margin between ca. 1220 and 1110 Ma although they note a lack of evidence for known North China orogenesis at this time. In terms of departing from this position, one possibility is that its departure is associated with early Neoproterozoic extension in northwest Laurentia.

#### 4.8 THE RECORD IMPLIES PLATE TECTONICS THROUGHOUT THE PROTEROZOIC

There is strong evidence both in Laurentia's geological and paleomagnetic record for differential plate tectonic motion between 2.2 and 1.8 Ga. The continued history of accretionary orogenesis and the evaluation of Laurentia's pole path in comparison to other continents from 1.8 Ga onward supports the continual operation of plate tectonics throughout the rest of the Proterozoic and Phanerozoic as well. While this evidence fits with the majority of interpretations of the timing of initiation of modern-style plate tectonics (see summary in Korenaga, 2013), there continue to be arguments proposing that a stagnant lid persisted through the Mesoproterozoic Era (1.6 to 1.0 Ga) and into the Neoproterozoic with plate tectonics not initiating until ca. 0.8 Ga (Hamilton, 2011; Stern and Miller, 2018). These arguments rest largely on the relative lack of Proterozoic low-temperature high-pressure metamorphic rocks such as blueschists that form in subduction zones (Stern et al., 2013). An alternative interpretation for this lack of blueschists in the Proterozoic is that such a shift in metamorphic regime is the predicted result of secular evolution of mantle chemistry rather than a harbinger of the onset of plate tectonics (Palin and White, 2015). While this line of evidence is intriguing, to argue that there was no differential plate tectonic motion in the Paleoproterozoic and Mesoproterozoic is to ignore a vast breadth and depth of geological and paleomagnetic data. From a paleomagnetic perspective, there is strong support for independent and differential motion of the Slave and Superior provinces as is illustrated in Figure 4. From a geological perspective, the Trans-Hudson orogenic cycle, the Grenville orogenic cycle, and the Appalachian orogenic cycle are all well-explained with a mobilistic interpretation that includes phases of accretionary followed by collisional orogenesis (Fig. 2). One could counter that this perspective results from a plate-tectonic-centric viewpoint that lacks creativity to see the record as resulting from other processes than modern-style plate tectonics. However,

in addition to the broad geological record showing an amalgamation of terranes as would be expected to arise through plate tectonics, there are also an obducted ophiolite as well as eclogites preserved in the Trans-Hudson orogen (Weller and St-Onge, 2017). These eclogites preserve evidence for high-pressure/low-temperature metamorphic conditions ca. 1.8 Ga. Similar to the Himalayan orogen, these rocks are interpreted to be the result of deep continental subduction and exhumation associated with convergent plate tectonics (Weller and St-Onge, 2017). Outside of Laurentia, there are examples of eclogites with geochemical affinity to oceanic crust such as that documented in the ca. 1.9 Ga Ubendian Belt of the Congo craton (Boniface et al., 2012).

Another perspective on Proterozoic tectonics, is that the record is one of intermittent subduction (Silver and Behn, 2008; O'Neill et al., 2013). In such a model, there are extended intervals with a stagnant lid alternating with intervals of differential plate motion. In particular, it has been argued that the Mesoproterozoic Era (1.6 to 1.0 Ga) is an interval when Earth was in a stagnant regime (Silver and Behn, 2008; O'Neill et al., 2013). The long-lived accretionary history of Laurentia following the amalgamation of the Archean provinces is difficult to reconcile with such an interpretation (Figs. 1 and 2).

An additional constraint supporting ongoing plate tectonics throughout the Proterozoic comes from the paleomagnetic record — in particular the paleomagnetic poles supported with baked contact tests (Fig. ??). In a stagnant lid regime, there would not be sufficient heat flow across the core-mantle boundary to sustain a geodynamo (Nimmo and Stevenson, 2000; Buffett, 2000). Baked contact tests indicate that, at the time of dike emplacement, there was an appreciable field such that both the cooling magma and the heated country rock in the vicinity of a dike were able to acquire a primary coherent magnetization direction. Additionally, since paleomagnetic poles are developed from many individual cooling units across a region, the similarity of the directions across an igneous province indicates that the magnetizations were dominantly acquired from the geomagnetic field rather than being influenced by local variable crustal magnetizations. Therefore, the record supports the persistence of a geomagnetic field through the Paleoproterozoic and Mesoproterozoic (Table 2) which implies active plate tectonics that enabled sufficient core-mantle boundary heat flow to power the geodynamo. This interpretation of a significant persistent geomagnetic field through much of the Proterozoic (with the potential exception of the Ediacaran; Bono et al., 2019) is further bolstered by estimates of paleointensity obtained from mafic dikes from Laurentia (e.g. Macouin et al., 2006) and elsewhere.

The record of these poles also show that there was progressive motion of Laurentia through the Proterozoic (Figs. 5 and 6). Using data from Laurentia alone, however, it is difficult to ascertain whether this motion is due to plate tectonic motion or rotation of the entire solid Earth through true polar wander. True polar wander can lead to changing position relative to the spin axis even with a stagnant lid. One interval when the Laurentian paleomagnetic record demands that some of the motion is through differential plate tectonics is in the latest Mesoproterozoic. At that time, the pole path is very well-resolved with many high-quality paleomagnetic poles between 1110 and 1070

Ma (Table 2; 3). The progression of the poles requires rotation about an Euler pole that is distinct from a great circle path which would result if the motion were solely due to true polar wander (Swanson-Hysell et al., 2019). These poles constrain rapid motion of Laurentia leading up to collisional orogenesis associated with the Grenvillian orogeny, as illustrated in Figure 8. These data provide strong evidence for differential plate motion at the time and are inconsistent with a stagnant lid. Rather, the orogenic cycle of the Mesoproterozoic bears similarity with that of the Paleozoic and reveals Laurentia to have been a central player in the building of amalgamated continents associated with Rodinia and Pangea.

## 4.9 CONCLUSION

The paleogeographic record of Laurentia is rich in constraints through the Precambrian both in terms of the geological and geochronological constraints on tectonism and the record of paleomagnetic poles. Data from the Slave and Superior provinces of Laurentia provide what is arguably the strongest evidence of differential plate tectonics in the Rhyacian and Orosirian Periods of the Paleoproterozoic Era (2.3 to 1.8 Ga) leading up to the collision of these terranes during the Trans-Hudson orogeny. The collisions of these and other Archean provinces led to the formation of the core of Laurentia. Subsequent crustal growth occurred through multiple intervals of accretionary orogenesis through the late Paleoproterozoic and Mesoproterozoic until the continent-continent collision of the Grenvillian orogeny that was ongoing at the Mesoproterozoic-Neoproterozoic boundary (1.0 Ga). The lead-up to this orogeny was associated with rapid plate motion of Laurentia from high latitudes towards the equator recorded by the Logan Loop and Keweenawan Track of paleomagnetic poles. Following, a return to high latitudes as constrained by paleomagnetic poles of the Grenville Loop, Laurentia straddled the equator at the time of Cryogenian Snowball Earth glaciation as part of the Rodinia supercontinent. Rifting and passive margin development then isolated Laurentia in the early Paleozoic Era. Subsequent accretionary and collisional orogenesis occurred associated with the Appalachian orogenic cycle with Laurentia first colliding with Avalonia-Baltica to become Laurussia and Laurussia then uniting with Gondwana to form Pangea. While the details of the conjugate continents are better reconstructed for this last Wilson cycle, the broad features of the Trans-Hudson, Grenvillian and Appalachian orogenic cycles bear similarities. In each case, accretionary collision of arc terranes was followed by continent-continent collision. The major difference is that the collisions of the Grenvillian and Appalachian orogenic cycles resulted in relatively minor crustal growth compared to the Trans-Hudson. Break-up following the Grenvillian and Appalachian orogenic cycles occurred along the same margin as collision while the major orogens of the Trans-Hudson orogenic cycle have remained sutured. As a result, Laurentia has been a formidable continent for the past 1.8 billion years. As can be seen in the Chapters on Archean paleogeography (Salminen et al., this volume), Nuna (Elming et al., this volume) and Rodinia (Evans et al., this volume), the constraints from Laurentia are at the center of paleogeographic models through the Precambrian and will continue to be as the next generation of paleogeographic models are developed.

## ACKNOWLEDGEMENTS

Many participants in the Nordic Paleomagnetism Workshop have contributed to the compilation and evaluation of the pole list utilized herein. Particular acknowledgement goes to David Evans for maintaining and distributing the compiled pole lists as well as additional efforts of Lauri Pesonen in maintaining the Paleomagia database (Veikkolainen et al., 2014). GPlates, and in particular the pyGPlates API, was utilized in this work (Müller et al., 2018). Figures were made using Matplotlib (Hunter, 2007) in conjunction with cartopy (Met Office, 2010 - 2015) and pmagpy (Tauxe et al., 2016) within an interactive Python environment (Pérez and Granger, 2007). The manuscript benefited from reviews from Athena Eyster, David Evans, and Lauri Pesonen as well as discussions with Francis Macdonald. This work was supported by NSF CAREER Grant EAR-1847277. The chapter text as well as code, data, and reconstructions used in this paper are openly available and licensed for any form of reuse with attribution (CC BY 4.0) in this repository: [https://github.com/Swanson-Hysell-Group/Laurentia\\_Paleogeography](https://github.com/Swanson-Hysell-Group/Laurentia_Paleogeography).

## GLOSSARY

**accretionary orogeny** Lithospheric deformation associated with the subduction of oceanic lithosphere and the addition of material from the downgoing plate such as island arcs.

**allochthonous** An adjective denoting that a rock or terrane originated in a position at significant distance from the lithospheric block that it is currently a part of.

**Archean** A geologic eon spanning from 4,000 to 2,500 million years ago (4 to 2.5 Ga)

**Archean province** A contiguous area of Archean continental lithosphere typically surrounded by Proterozoic orogens inferred to be suture zones (e.g. Superior province).

**Canadian shield** Large area of exposed Precambrian rock of Laurentia, or rock covered by thin soil, that is well-exposed due to Pleistocene glaciation erosion

**collisional orogeny** Lithospheric deformation resulting from the collision of two significant provinces of continental lithosphere.

**conjugate** Adjective referring to continents or continental margins that were previously conjoined.

**craton** The stable and relatively immobile continental lithosphere in the interior of continents. In this chapter, craton is predominantly used in reference to Laurentia which formed through the collision of Archean provinces and grew further through subsequent accretionary and collisional orogenesis.

**Elzevirian orogen** The orogen resulting from the Mesoproterozoic Elzevirian orogeny when there was accretion of arc terranes to eastern Laurentia.

**evaporite** Minerals that crystallize from water that becomes supersaturated in salts through evaporation.

**Ga** Giga annum, one billion ( $10^9$ ) years. This term is used as an abbreviation for “billions of years before present.”

**geocentric axial dipole hypothesis** The hypothesis that when it is time-averaged, Earth’s magnetic field is dominantly a dipole aligned with the spin axis.

**Granite-rhyolite province** A geologic province that comprises widespread Mesoproterozoic rhyolite and granite extending from southeastern Ontario, Canada to west Texas, USA.

**Grenvillian orogen** An orogen resulting from collision orogeny between Laurentia and conjugate continent(s) near the end of the Mesoproterozoic.

**Hadley cell** Large-scale atmospheric circulation where air rises near the equator, flows poleward, and descends in the subtropics. This circulation drives convective tropical precipitation and the dry down-welling air leads to aridity in the subtropics.

**Hearne province** An Archean province of Laurentia extending from southern Alberta, Canada to Hudson Bay. It is framed by the Rae province to the northwest and the Trans-Hudson orogen to the southeast. It is also referred to as the Hearne craton.

**hematite** An iron oxide mineral with a formula of  $\text{Fe}_2\text{O}_3$  that commonly holds magnetization in geologic materials, particularly oxidized sedimentary rocks.

**juvenile** Rocks that have formed through melt recently extracted from the mantle.

**Laurentia** The Precambrian cratonic core of the North America continent and Greenland that formed through the amalgamation of Archean provinces in the Paleoproterozoic.

**large igneous province (LIP)** Voluminous and rapidly emplaced volcanics and intrusions that are typically of mafic composition. These provinces are often interpreted to be due to decompression melting of an upwelling mantle plume.

**lithosphere** The rigid outermost layer of the Earth that is broken into tectonic plates and responds to the emplacement of a load by flexural bending.

**Ma** Mega annum, one million ( $10^6$ ) years. This term is used as an abbreviation for “millions of years before present.”

**Manikewan Ocean** An ocean basin interpreted to have existed between the Slave+Rae+Hearne+North Atlantic provinces and Superior province that closed leading up to the Trans-Hudson orogeny.

**Mazatzal orogen** An orogen resulting from latest Paleoproterozoic accretion of volcanic arc and back-arc terranes with southern Laurentia.

**Medicine Hat province** An Archean province of Laurentia extending from northern Montana, USA into southern Alberta and Saskatchewan, Canada. It is framed by a suture with the Hearne province to the north, the Trans-Hudson orogen to the east, and the Great Falls tectonic zone to the south. It is also referred to as the Medicine Hat block

**Mesoproterozoic** A geologic era spanning from 1,600 to 1,000 million years ago.

**Meta Incognita province** A province of Archean basement rocks that comprises most of southern Baffin Island. It is also referred to as the Meta Incognita microcontinent.

**Midcontinent Rift** A major Mesoproterozoic intracratonic rift where there was co-location of large igneous province magmatism and extension in Laurentia’s interior centered on the Lake Superior region.

**monazite** A phosphate mineral ( $\text{Ce},\text{La},\text{Nd},\text{Th})(\text{PO}_4,\text{SiO}_4)$  found as an accessory phase in metamorphic rocks that can be targeted by U-Pb geochronology to date metamorphic events.

**Nagssugtoqidian orogen** An orogen resulting from the Paleoproterozoic collision between the Rae and North Atlantic provinces.

**Neoproterozoic** A geologic era spanning from 1,000 to 541 million years ago.

**North Atlantic province** An Archean province of Laurentia in southernmost Greenland and northeastern Labrador, Canada. It is also referred to as the North Atlantic craton.

**Nuna** A hypothesized supercontinent interpreted to have formed late in the Paleoproterozoic era and broke apart in the middle of the Mesoproterozoic.

**orogen** A region of lithosphere that has undergone deformation during a mountain-building event (an orogeny).

**paleolatitude** The past latitude of a given point on Earth’s surface at a given time.

**paleomagnetic pole** A calculated position from paleomagnetic data that is interpreted to correspond to the ancient position of Earth’s spin axis (the north pole) through application of the geocentric axial dipole hypothesis. The uncertainty on the pole position is given as a circle with a radius of a given angle ( $A_{95}$ ).

**Paleoproterozoic** A geologic era spanning from 2,500 to 1,600 million years ago.

**Penokean orogen** An orogen resulting from Paleoproterozoic accretion of an oceanic arc and the Marshfield terrane continental block along the southern margin of the Superior province.

**Phanerozoic** A geologic eon spanning from 541 million years ago to the present day.

**Picuris orogen** An orogen resulting from a Mesoproterozoic orogeny interpreted from metamorphic rocks with Mesoproterozoic-aged protoliths in northern New Mexico, USA.

**Precambrian** A commonly used informal term to refer to geologic time prior to the Cambrian Period that started 541 million years ago.

**Proterozoic** A geologic eon spanning from 2,500 to 541 million years ago.

**province** A spatial entity with a shared geologic history. The term is used in this chapter to refer to Archean provinces that moved as independent cratonic blocks prior to Laurentia’s amalgamation (e.g. Superior province). It is also used to refer to zones of crustal growth associated with orogens and the products of contemporaneous magmatic activity (large igneous provinces).

**Rae province** An Archean province of Laurentia extending the region of Lake Athabasca northeast to northern Baffin Island in arctic Canada. It is framed by the Thelon orogen to the west, the Taltson orogen to the southwest and the Hearne province to the east. It is also referred to as the Rae craton.

**Rodinia** A hypothesized supercontinent interpreted to have formed late in the Mesoproterozoic era and broke apart in the middle of the Neoproterozoic.

**Slave province** An Archean province of Laurentia extending to the north from the region of Great Slave Lake in northern Canada. It is framed by the Thelon orogen to the east and the Great Bear Arc to the west. It is also referred to as the Slave craton.

**Shawinigan orogen** The orogen resulting from the Mesoproterozoic Shawinigan orogeny when there was accretion of terranes to eastern Laurentia.

**Snowbird orogen** An orogen resulting from Paleoproterozoic collision between the Rae and Hearne provinces prior to the Trans-Hudson orogeny. The Snowbird tectonic zone is part of the orogen.

**Superior province** The largest Archean province of Laurentia framed by the Trans-Hudson orogen to the west, the Grenvillian orogen to the east and the Penokean orogen to the south. It is also referred to as the Superior craton.

**Thelon orogen** An orogen resulting from the Paleoproterozoic collision orogeny between the Slave and Rae provinces.

**thermal remanent magnetization** Magnetization acquired by magnetic minerals rocks as they cool following crystallization from magma.

**Torngat orogen** An orogen resulting from the Paleoproterozoic collision orogeny between the Meta Incognita and North Atlantic provinces.

**Trans-Hudson orogen** An orogen resulting from the Paleoproterozoic collision between the composite Slave+Rae+Hearne provinces and the Superior province.

**Wopmay orogen** An orogen resulting from Paleoproterozoic collision between the Hottah terrane, a continental magmatic arc, and the west margin of the Slave province.

**Wyoming province** An Archean province of Laurentia underlying much of Wyoming, USA and southeast Montana, USA. It is framed by the Trans-Hudson orogen to the east (sometimes referred to as the Black Hills orogen within the USA) and the Great Falls tectonic zone to the north. It is also referred to as the Wyoming craton.

**Yavapai orogen** An orogen resulting from Paleoproterozoic collision and accretion of oceanic arc terranes with southern Laurentia.

**zircon** A nesosilicate mineral with the chemical name of zirconium silicate and a chemical formula of  $ZrSiO_4$ .

## REFERENCES

- Abrahamsen, N. and Van Der Voo, R., 1987. Palaeomagnetism of middle Proterozoic (c. 1.25 Ga) dykes from central North Greenland. *Geophysical Journal International*, v. 91, p. 597–611, doi: 10.1111/j.1365-246x.1987.tb01660.x.
- Abrajevitch, A. and Van der Voo, R., 2010. Incompatible Ediacaran paleomagnetic directions suggest an equatorial geomagnetic dipole hypothesis. *Earth and Planetary Science Letters*, v. 293, p. 164–170, doi: 10.1016/j.epsl.2010.02.038.
- Aronoff, R. F., Andronicos, C. L., Vervoort, J. D., and Hunter, R. A., 2016. Redefining the metamorphic history of the oldest rocks in the southern Rocky Mountains. *Geological Society of America Bulletin*, v. 128, p. 1207–1227, doi: 10.1130/b31455.1.
- Bates, M. P. and Halls, H. C., 1991. Broad-scale Proterozoic deformation of the central Superior Province revealed by paleomagnetism of the 2.45 Ga Matachewan dyke swarm. *Canadian Journal of Earth Sciences*, v. 28, p. 1780–1796, doi: 10.1139/e91-159.
- Berman, R., Davis, A., and Pehrsson, S., 2007. Collisional Snowbird tectonic zone resurrected: Growth of Laurentia during the 1.9 Ga accretionary phase of the Hudsonian orogeny. *Geology*, v. 35, p. 911–914, doi: 10.1130/G23771A.1.
- Bickford, M., Van Schmus, W., Karlstrom, K., Mueller, P., and Kamennov, G., 2015. Mesoproterozoic-trans-Laurentian magmatism: A synthesis of continent-wide age distributions, new SIMS U-Pb ages, zircon saturation temperatures, and Hf and Nd isotopic compositions. *Precambrian Research*, v. 265, p. 286–312, doi: 10.1016/j.precamres.2014.11.024.
- Bond, G., Nickleson, P., and Komitz, M., 1984. Breakup of a supercontinent between 625 and 555 Ma: new evidence and implications for continental histories. *Earth and Planetary Science Letters*, v. 70, p. 325–345, doi: 10.1016/0012-821X(84)90017-7.
- Boniface, N., Schenk, V., and Appel, P., 2012. Paleoproterozoic eclogites of MORB-type chemistry and three Proterozoic orogenic cycles in the Ubendian Belt (Tanzania): Evidence from monazite and zircon geochronology, and geochemistry. *Precambrian Research*, v. 192–195, p. 16–33, doi: 10.1016/j.precamres.2011.10.007.
- Bono, R. K. and Tarduno, J. A., 2015. A stable Ediacaran Earth recorded by single silicate crystals of the ca. 565 Ma Sept-Îles intrusion. *Geology*, v. 43, p. 131–134, doi: 10.1130/G36247.1.
- Bono, R. K., Tarduno, J. A., Nimmo, F., and Cottrell, R. D., 2019. Young inner core inferred from Ediacaran ultra-low geomagnetic field intensity. *Nature Geoscience*, v. 12, p. 143–147, doi: 10.1038/s41561-018-0288-0.
- Books, K., 1972. Paleomagnetism of some Lake Superior Keweenawan rocks. *U.S. Geological Survey Professional Paper*, v. P 0760, p. 1–42.
- Borradaile, G. and Middleton, R., 2006. Proterozoic paleomagnetism in the Nipigon Embayment of northern Ontario: Pillar Lake Lava, Wawieg Troctolite and Gunflint Formation tuffs. *Precambrian Research*, v. 144, p. 69–91, doi: 10.1016/j.precamres.2005.10.007.
- Brown, L. L. and McEnroe, S. A., 2012. Paleomagnetism and magnetic mineralogy of Grenville metamorphic and igneous rocks, Adirondack Highlands, USA. *Precambrian Research*, v. 212–213, p. 57–74, doi: 10.1016/j.precamres.2012.04.012.
- Brown, M., Torsvik, T., and Pesonen, L., 2018. Nordic workshop takes on major puzzles of paleomagnetism. *Eos*, v. 99, doi: 10.1029/2018eo094671.
- Buchan, K., Mertanen, S., Park, R., Pesonen, L., Elming, S. A., Abrahamsen, N., and Bylund, G., 2000. Comparing the drift of Laurentia and Baltica in the Proterozoic: the importance of key paleomagnetic poles. *Tectonophysics*, v. 319, p. 167–198, doi: 10.1016/S0040-1951(00)00032-9.
- Buchan, K. L., LeCheminant, A. N., and van Breemen, O., 2009. Paleomagnetism and U–Pb geochronology of the Lac de Gras diabase dyke swarm, Slave Province, Canada: implications for relative drift of Slave and Superior provinces in the Paleoproterozoic. *Canadian Journal of Earth Sciences*, v. 46, p. 361–379, doi: 10.1139/e09-026.
- Buchan, K. L., LeCheminant, A. N., and van Breemen, O., 2012. Malley diabase dykes of the Slave craton, Canadian Shield: U–Pb age, paleomagnetism, and implications for continental reconstructions in the early Paleoproterozoic. *Canadian Journal of Earth Sciences*, v. 49, p. 435–454, doi: 10.1139/e11-061.
- Buchan, K. L., Mitchell, R. N., Bleeker, W., Hamilton, M. A., and LeCheminant, A. N., 2016. Paleomagnetism of ca. 2.13–2.11 Ga Indin and ca. 1.885 Ga Ghost dyke swarms of the Slave craton: Implications for the Slave craton APW path and relative drift of Slave, Superior and Siberian cratons in the Paleoproterozoic. *Precambrian Research*, v. 275, p. 151–175, doi: 10.1016/j.precamres.2016.01.012.
- Buchan, K. L., Mortensen, J. K., and Card, K. D., 1993. Northeast-trending early Proterozoic dykes of southern Superior Province: multiple episodes of emplacement recognized from integrated paleomagnetism and U–Pb geochronology. *Canadian Journal of Earth Sciences*, v. 30, p. 1286–1296, doi: 10.1139/e93-110.
- Buffett, B. A., 2000. Earth's core and the geodynamo. *Science*, v. 288, p. 2007–2012, doi: 10.1126/science.288.5473.2007.
- Burls, N. J. and Fedorov, A. V., 2017. Wetter subtropics in a warmer world: Contrasting past and future hydrological cycles. *Proceedings of the National Academy of Sciences*, v. 114, p. 12,888–12,893, doi: 10.1073/pnas.1703421114.
- Burton, W. C. and Southworth, S., 2010. A model for Iapetan rifting of Laurentia based on Neoproterozoic dikes and related rocks. From Rodinia to Pangea: The Lithotectonic Record of the Appalachian Region, p. 455–476, doi: 10.1130/2010.1206(20).

- Cannon, W. F., 1992. The Midcontinent rift in the Lake Superior region with emphasis on its geodynamic evolution. *Tectonophysics*, v. 213, p. 41–48, doi:10.1016/0040-1951(92)90250-A.
- Cawood, P. A. and Pisarevsky, S. A., 2017. Laurentia-Baltica–Amazonia relations during Rodinia assembly. *Precambrian Research*, v. 292, p. 386–397, doi:10.1016/j.precamres.2017.01.031.
- Chiarenzelli, J., Lupulescu, M., Thern, E., and Cousens, B., 2011. Tectonic implications of the discovery of a Shawinigan ophiolite (Pyrites Complex) in the Adirondack Lowlands. *Geosphere*, v. 7, p. 333–356, doi:10.1130/ges00608.1.
- Condit, C. B., Mahan, K. H., Ault, A. K., and Flowers, R. M., 2015. Foreland-directed propagation of high-grade tectonism in the deep roots of a Paleoproterozoic collisional orogen, SW Montana, USA. *Lithosphere*, v. 7, p. 625–645, doi:10.1130/l460.1.
- Corrigan, D., Pehrsson, S., Wodicka, N., and de Kemp, E., 2009. The Palaeoproterozoic Trans-Hudson Orogen: a prototype of modern accretionary processes. *Geological Society, London, Special Publications*, v. 327, p. 457–479, doi:10.1144/sp327.19.
- Dahl, P. S., Holm, D. K., Gardner, E. T., Hubacher, F. A., and Foland, K. A., 1999. New constraints on the timing of Early Proterozoic tectonism in the Black Hills (South Dakota), with implications for docking of the Wyoming province with Laurentia. *Geological Society of America Bulletin*, v. 111, p. 1335–1349, doi:10.1130/0016-7606(1999)111<1335:ncotto>2.3.co;2.
- Daniel, C. G., Pfeifer, L. S., Jones, J. V., and McFarlane, C. M., 2013. Detrital zircon evidence for non-Laurentian provenance, Mesoproterozoic (ca. 1490–1450 Ma) deposition and orogenesis in a reconstructed orogenic belt, northern New Mexico, USA: Defining the Picuris orogeny. *Geological Society of America Bulletin*, v. 125, p. 1423–1441, doi:10.1130/b30804.1.
- de Kock, M. O., Luskin, C. R., Djeutchou, C., and Wabo, H., 2021. The Precambrian drift history and paleogeography of the Kalahari Craton. In Pesonen, L. J., Evans, D. A. D., Elming, S. Å., Salminen, J. M., and Veikkolainen, T., eds., *Ancient Supercontinents and the Paleogeography of the Earth*, Elsevier.
- Dehler, C., Gehrels, G., Porter, S., Heizler, M., Karlstrom, K., Cox, G., Crossey, L., and Timmons, M., 2017. Synthesis of the 780–740 Ma Chuar, Uinta Mountain, and Pahrump (ChUMP) groups, western USA: Implications for Laurentia-wide cratonic marine basins. *Geological Society of America Bulletin*, v. 129, p. 607–624, doi:10.1130/b31532.1.
- Denysyn, S. W., Davis, D. W., and Halls, H. C., 2009a. Paleomagnetism and U–Pb geochronology of the Clarence Head dykes, Arctic Canada: orthogonal emplacement of mafic dykes in a large igneous province. *Canadian Journal of Earth Sciences*, v. 46, p. 155–167, doi:10.1139/E09-011.
- Denysyn, S. W., Halls, H. C., Davis, D. W., and Evans, D. A. D., 2009b. Paleomagnetism and U–Pb geochronology of Franklin dykes in High Arctic Canada and Greenland: a revised age and paleomagnetic pole constraining block rotations in the Nares Strait region. *Canadian Journal of Earth Sciences*, v. 46, p. 689–705, doi:10.1139/E09-042.
- Dickerson, P. W. and Keller, M., 1998. The Argentine Precordillera: its odyssey from the Laurentian Ouachita margin towards the Sierras Pampeanas of Gondwana. *Geological Society, London, Special Publications*, v. 142, p. 85–105, doi:10.1144/gsl.sp.1998.142.01.05.
- Diener, J. F., White, R. W., Link, K., Dreyer, T. S., and Moodley, A., 2013. Clockwise, low- metamorphism of the Aus granulite terrain, southern Namibia, during the Mesoproterozoic Namaqua Orogeny. *Precambrian Research*, v. 224, p. 629–652, doi:10.1016/j.precamres.2012.11.009.
- Donadini, F., Pesonen, L. J., Korhonen, K., Deutsch, A., and Harlan, S. S., 2011. Paleomagnetism and paleointensity of the 1.1 Ga old diabase sheets from central Arizona. *Geophysica*, v. 47, p. 3–30.
- Elming, S. Å., D’Agrella-Filho, M. S., Page, L. M., Tohver, E., Trindade, R. I. F., Pacca, I. I. G., Gerald, M. C., and Teixeira, W., 2009. A palaeomagnetic and 40Ar/39Ar study of late precambrian sills in the SW part of the Amazonian craton: Amazonia in the Rodinia reconstruction. *Geophysical Journal International*, v. 178, p. 106–122.
- Elming, S. Å., Salminen, J., and Pesonen, L. J., 2021. Paleo-Mesoproterozoic Nuna supercycle. In Pesonen, L. J., Evans, D. A. D., Elming, S. Å., Salminen, J. M., and Veikkolainen, T., eds., *Ancient Supercontinents and the Paleogeography of the Earth*, Elsevier.
- Elston, D. P., Enkin, R. J., Baker, J., and Kisilevsky, D. K., 2002. Tightening the Belt: Paleomagnetic-stratigraphic constraints on deposition, correlation, and deformation of the Middle Proterozoic (ca. 1.4 Ga) Belt-Purcell Supergroup, United States and Canada. *GSA Bulletin*, v. 114, p. 619–638, doi:10.1130/0016-7606(2002)114<0619:TTBPSC>2.0.CO;2.
- Emslie, R. F., Irving, E., and Park, J. K., 1976. Further paleomagnetic results from the Michikamau Intrusion, Labrador. *Canadian Journal of Earth Sciences*, v. 13, p. 1052–1057, doi:10.1139/e76-108.
- Ernst, R. and Buchan, K., 1993. Paleomagnetism of the Abitibi dike swarm, southern Superior Province, and implications for the Logan Loop. *Canadian Journal of Earth Science*, v. 30, p. 1886–1897, doi:10.1139/e93-167.
- Eugster, H. P., 1980, Chapter 15 Lake Magadi, Kenya, and Its Precursors. In Nissenbaum, A., ed., *Developments in Sedimentology*, Elsevier, p. 195–232, doi:10.1016/s0070-4571(08)70239-5.
- Evans, D., 2003. True polar wander and supercontinents. *Tectonophysics*, v. 362, p. 303–320, doi:10.1016/S0040-1951(02)000642-X.
- Evans, D., 2006. Proterozoic low orbital obliquity and axial-dipolar geomagnetic field from evaporite palaeolatitudes. *Nature*, v. 444, p. 51–55, doi:10.1038/nature05203.
- Evans, D. A. D., 2013. Reconstructing pre-Pangean supercontinents. *Geological Society of America Bulletin*, v. 125, p. 1735–1751, doi:10.1130/B30950.1.
- Evans, D. A. D. and Halls, H. C., 2010. Restoring Proterozoic deformation within the Superior craton. *Precambrian Research*, v. 183, p. 474 – 489, doi:10.1016/j.precamres.2010.02.007.
- Evans, D. A. D. and Mitchell, R. N., 2011. Assembly and breakup of the core of Paleoproterozoic–Mesoproterozoic supercontinent Nuna. *Geology*, v. 39, p. 443–446, doi:10.1130/G31654.1.
- Evans, D. A. D., Pesonen, L. J., Eglington, B. M., Elming, S.-Å., Gong, Z., Li, Z.-X., McCausland, P., Meert, J., Mertanen, S., Pisarevsky, S., Pivarunas, A., Salminen, J., Swanson-Hysell, N., Torsvik, T., Trindade, R., Veikkolainen, T., and Zhang, S., 2021. An expanding list of reliable paleomagnetic poles for Precambrian tectonic reconstructions. In Pesonen, L. J., Evans, D. A. D., Elming, S. Å., Salminen, J. M., and Veikkolainen, T., eds., *Ancient Supercontinents and the Paleogeography of the Earth*, Elsevier.
- Evans, D. A. D. and Pisarevsky, S. A., 2008. Plate tectonics on early Earth? weighing the paleomagnetic evidence. *Geological Society of America Special Papers*, v. 440, p. 249–263, doi:10.1130/2008.2440(12).
- Evans, K. A., McCuaig, T. C., Leach, D., Angerer, T., and Hagemann, S. G., 2013. Banded iron formation to iron ore: A record of the evolution of earth environments?. *Geology*, v. 41, p. 99–102.

- Evans, K. V., Aleinikoff, J. N., Obradovich, J. D., and Fanning, C. M., 2000. SHRIMP U-Pb geochronology of volcanic rocks, Belt Supergroup, western Montana: evidence for rapid deposition of sedimentary strata. *Canadian Journal of Earth Sciences*, v. 37, p. 1287–1300, doi:10.1139/e00-036.
- Evans, M. E. and Bingham, D. K., 1973. Paleomagnetism of the Precambrian Martin Formation, Saskatchewan. *Canadian Journal of Earth Sciences*, v. 10, p. 1485–1493, doi:10.1139/e73-141.
- Evans, M. E. and Hoye, G. S., 1981. Paleomagnetic results from the lower Proterozoic rocks of Great Slave Lake and Bathurst Inlet areas, Northwest Territories. In *Proterozoic Basins of Canada*; Geological Survey of Canada, Paper 81-10, Natural Resources Canada/ESS/Scientific and Technical Publishing Services, doi:10.4095/109374.
- Eyster, A., Weiss, B. P., Karlstrom, K., and Macdonald, F. A., 2019. Paleomagnetism of the Chuar Group and evaluation of the late Tonian Laurentian apparent polar wander path with implications for the makeup and breakup of Rodinia. *GSA Bulletin*, doi:10.1130/b32012.1.
- Fahrig, W. and Bridgwater, D., 1976. Late Archean-early Proterozoic paleomagnetic pole positions from west Greenland. In Windley, B., ed., *Early History of the Earth*, Wiley, p. 427–442.
- Fahrig, W. F. and Jones, D. L., 1976. The paleomagnetism of the Helikian Mistastin pluton, Labrador, Canada. *Canadian Journal of Earth Sciences*, v. 13, p. 832–837, doi:10.1139/e76-086.
- Fairchild, L. M., Swanson-Hysell, N. L., Ramezani, J., Sprain, C. J., and Bowring, S. A., 2017. The end of Midcontinent Rift magmatism and the paleogeography of Laurentia. *Lithosphere*, v. 9, p. 117–133, doi:10.1130/L580.1.
- Fisher, C. M., Loewy, S. L., Miller, C. F., Berquist, P., Van Schmus, W. R., Hatcher, R. D., Wooden, J. L., and Fullagar, P. D., 2010. Whole-rock Pb and Sm-Nd isotopic constraints on the growth of southeastern Laurentia during Grenvillian orogenesis. *Geological Society of America Bulletin*, v. 122, p. 1646–1659, doi:10.1130/b30116.1.
- Gala, M. G., Symons, D. T. A., and Palmer, H. C., 1995. Paleomagnetism of the Jan Lake Granite, Trans-Hudson Orogen. *Saskatchewan Geological Survey Summary of Investigations*, v. 95-4.
- Gibson, T. M., Shih, P. M., Cumming, V. M., Fischer, W. W., Croxford, P. W., Hodgsiss, M. S., Wörndle, S., Creaser, R. A., Rainbird, R. H., Skulski, T. M., and et al., 2018. Precise age of Bangiomorpha pubescens dates the origin of eukaryotic photosynthesis. *Geology*, doi:10.1130/g39829.1.
- Gower, C. F., Ryan, A. B., and Rivers, T., 1990. Mid-Proterozoic Laurentia-Baltica: An overview of its geological evolution and a summary of the contributions made by this volume. In Gower, C. F., Rivers, T., and Ryan, A. B., eds., *Mid-Proterozoic Laurentia-Baltica*, Geological Association of Canada, Special Paper.
- Grimes, S. W. and Copeland, P., 2004. Thermochronology of the Grenville Orogeny in west Texas. *Precambrian Research*, v. 131, p. 23–54, doi:10.1016/j.precamres.2003.12.004.
- Halls, H., 1974. A paleomagnetic reversal in the Osler Volcanic Group, northern Lake Superior. *Canadian Journal of Earth Science*, v. 11, p. 1200–1207, doi:10.1139/e74-113.
- Halls, H. C., 2015. Paleomagnetic evidence for ~4000 km of crustal shortening across the 1 Ga Grenville orogen of North America. *Geology*, v. 43, p. 1051–1054, doi:10.1130/G37188.1.
- Halls, H. C., Davis, D. W., Stott, G. M., Ernst, R. E., and Hamilton, M. A., 2008. The Paleoproterozoic Marathon Large Igneous Province: New evidence for a 2.1 Ga long-lived mantle plume event along the southern margin of the North American Superior Province. *Precambrian Research*, v. 162, p. 327–353, doi:10.1016/j.precamres.2007.10.009.
- Halls, H. C., Hamilton, M. A., and Denysyn, S. W., 2011. The Melville Bugt dyke swarm of Greenland: A connection to the 1.5–1.6 Ga Fennoscandian rapakivi granite province?. In Srivastava, R. K., ed., *Dyke Swarms: Keys for Geodynamic Interpretation*, Springer Berlin Heidelberg, p. 509–535, doi:10.1007/978-3-642-12496-9\_27.
- Halls, H. C. and Hanes, J. A., 1999. Paleomagnetism, anisotropy of magnetic susceptibility, and argon–argon geochronology of the Clearwater anorthosite, Saskatchewan, Canada. *Tectonophysics*, v. 312, p. 235–248, doi:10.1016/s0040-1951(99)00166-3.
- Halls, H. C., Lovette, A., Hamilton, M., and Söderlund, U., 2015. A paleomagnetic and U-Pb geochronology study of the western end of the Grenville dyke swarm: Rapid changes in paleomagnetic field direction at ca. 585 Ma related to polarity reversals?. *Precambrian Research*, v. 257, p. 137–166, doi:10.1016/j.precamres.2014.11.029.
- Halverson, G. P., Porter, S. M., and Gibson, T. M., 2018. Dating the late Proterozoic stratigraphic record. *Emerging Topics in Life Sciences*, v. 2, p. 137–147, doi:10.1042/etls20170167.
- Hamilton, W. B., 2011. Plate tectonics began in Neoproterozoic time, and plumes from deep mantle have never operated. *Lithos*, v. 123, p. 1–20, doi:10.1016/j.lithos.2010.12.007.
- Harlan, S., 1993. Paleomagnetism of Middle Proterozoic diabase sheets from central Arizona. *Canadian Journal of Earth Science*, v. 30, p. 1415–1426, doi:10.1139/e93-122.
- Harlan, S., Geissman, J., and Snee, L., 1997. Paleomagnetic and  $^{40}\text{Ar}/^{39}\text{Ar}$  geochronologic data from late Proterozoic mafic dykes and sills, Montana and Wyoming. USGS Professional Paper, v. 1580, p. 1–16.
- Harlan, S. S. and Geissman, J. W., 1998. Paleomagnetism of the middle Proterozoic Electra Lake Gabbro, Needle Mountains, southwestern Colorado. *Journal of Geophysical Research: Solid Earth*, v. 103, p. 15,497–15,507, doi:10.1029/98jb01350.
- Harlan, S. S., Geissman, J. W., and Snee, L. W., 2008. Paleomagnetism of Proterozoic mafic dikes from the Tobacco Root Mountains, southwest Montana. *Precambrian Research*, v. 163, p. 239–264, doi:10.1016/j.precamres.2007.12.002.
- Harlan, S. S., Snee, L. W., Geissman, J. W., and Brearley, A. J., 1994. Paleomagnetism of the Middle Proterozoic Laramie anorthosite complex and Sherman Granite, southern Laramie Range, Wyoming and Colorado. *Journal of Geophysical Research: Solid Earth*, v. 99, p. 17,997–18,020, doi:10.1029/94jb00580.
- Henry, S., Mauk, F., and Van der Voo, R., 1977. Paleomagnetism of the upper Keweenawan sediments: Nonesuch Shale and Freda Sandstone. *Canadian Journal of Earth Science*, v. 14, p. 1128–1138, doi:10.1139/e77-103.
- Hietanen, A., 1967. Scapolite in the Belt series in the St. Joe-Clearwater region, Idaho. *GSA Special Papers*, v. 86, doi:10.1130/spe86.
- Hildebrand, R. S., Hoffman, P. F., and Bowring, S. A., 2009. The Calderian orogeny in Wopmay orogen (1.9 Ga), northwestern Canadian Shield. *Geological Society of America Bulletin*, v. 122, p. 794–814, doi:10.1130/B26521.1.
- Hnat, J. S., van der Pluijm, B. A., and Van der Voo, R., 2006. Primary curvature in the Mid-Continent Rift: Paleomagnetism of the Portage Lake Volcanics (northern Michigan, USA). *Tectonophysics*, v. 425, p. 71–82, doi:10.1016/j.tecto.2006.07.006.
- Hoffman, P., 1991. Did the breakout of Laurentia turn Gondwana inside out?. *Science*, v. 252, p. 1409–1412, doi:10.1126/science.252.5011.1409.

- Hoffman, P. F., 1988. United plates of America, the birth of a craton: Early Proterozoic assembly and growth of Laurentia. *Annual Review of Earth and Planetary Sciences*, v. 16, p. 543–603, doi:10.1146/annurev.ea.16.050188.002551.
- Hoffman, P. F., 1989. Speculations on Laurentia's first gigayear (2.0 to 1.0 Ga). *Geology*, v. 17, p. 135–138, doi:10.1130/0091-7613(1989)017<0135:SOLSGF>2.3.CO;2.
- Hoffman, P. F., Halverson, G. P., Domack, E. W., Maloof, A. C., Swanson-Hysell, N. L., and Cox, G. M., 2012. Cryogenian glaciations on the southern tropical paleomargin of Laurentia (NE Svalbard and East Greenland), and a primary origin for the upper Russøya (Islay) carbon isotope excursion. *Precambrian Research*, v. 206–207, p. 137–158, doi:10.1016/j.precamres.2012.02.018.
- Holm, D. K., Van Schmus, W. R., MacNeill, L. C., Boerboom, T. J., Schweitzer, D., and Schneider, D., 2005. U-Pb zircon geochronology of Paleoproterozoic plutons from the northern midcontinent, USA: Evidence for subduction flip and continued convergence after geon 18 Penokean orogenesis. *Geological Society of America Bulletin*, v. 117, p. 259–275, doi:10.1130/b25395.1.
- Hrncir, J., Karlstrom, K., and Dahl, P., 2017. Wyoming on the run—Toward final Paleoproterozoic assembly of Laurentia: COMMENT. *Geology*, v. 45, p. e411–e411, doi:10.1130/g38826c.1.
- Hunter, J. D., 2007. Matplotlib: A 2D graphics environment. *Computing in Science & Engineering*, v. 9, p. 90–95, doi:10.1109/MCSE.2007.55.
- Hynes, A. and Rivers, T., 2010. Protracted continental collision — evidence from the Grenville Orogen. *Canadian Journal of Earth Sciences*, v. 47, p. 591–620, doi:10.1139/e10-003.
- Irving, E., 2004. Early Proterozoic geomagnetic field in western Laurentia: implications for paleolatitudes, local rotations and stratigraphy. *Precambrian Research*, v. 129, p. 251–270, doi:10.1016/j.precamres.2003.10.002.
- Irving, E. and McGlynn, J. C., 1979. Palaeomagnetism in the Coronation Geosyncline and arrangement of continents in the middle Proterozoic. *Geophysical Journal International*, v. 58, p. 309–336, doi:10.1111/j.1365-246X.1979.tb01027.x.
- Irving, E. and Park, J. K., 1972. Hairpins and superintervals. *Canadian Journal of Earth Sciences*, v. 9, p. 1318–1324, doi:10.1139/e72-115.
- Jefferson, C. W. and Parrish, R. R., 1989. Late Proterozoic stratigraphy, U-Pb zircon ages, and rift tectonics, Mackenzie Mountains, northwestern Canada. *Canadian Journal of Earth Sciences*, v. 26, p. 1784–1801, doi:10.1139/e89-151.
- Johnson, T. A., Vervoort, J. D., Ramsey, M. J., Southworth, S., and Mulcahy, S. R., 2020. Tectonic evolution of the Grenville Orogen in the central Appalachians. *Precambrian Research*, v. 346, doi:10.1016/j.precamres.2020.105740.
- Jones, D. S., Maloof, A. C., Hurtgen, M. T., Rainbird, R. H., and Schrag, D. P., 2010. Regional and global chemostratigraphic correlation of the early Neoproterozoic Shaler Supergroup, Victoria Island, Northwestern Canada. *Precambrian Research*, v. 181, p. 43–63, doi:10.1016/j.precamres.2010.05.012.
- Jones, J. V., Daniel, C. G., and Doe, M. F., 2015. Tectonic and sedimentary linkages between the Belt-Purcell basin and southwestern Laurentia during the Mesoproterozoic, ca. 1.60–1.40 Ga. *Lithosphere*, v. 7, p. 465–472, doi:10.1130/l1438.1.
- Kah, L., Lyons, T., and Chesley, J., 2001. Geochemistry of a 1.2 Ga carbonate-evaporite succession, northern Baffin and Bylot Islands: implications for Mesoproterozoic marine evolution. *Precambrian Research*, v. 111, p. 203–234, doi:10.1016/S0301-9268(01)00161-9.
- Karlstrom, K. E., Ahall, K.-I., Harlan, S. S., Williams, M. L., McLellan, J., and Geissman, J. W., 2001. Long-lived (1.8–1.0 Ga) convergent orogen in southern Laurentia, its extensions to Australia and Baltica, and implications for refining Rodinia. *Precambrian Research*, v. 111, p. 5–30, doi:10.1016/S0301-9268(01)00154-1.
- Karlstrom, K. E. and Bowring, S. A., 1988. Early Proterozoic assembly of tectonostratigraphic terranes in southwestern North America. *The Journal of Geology*, v. 96, p. 561–576, doi:10.1086/629252.
- Kasbohm, J., Evans, D. A. D., Panzik, J. E., Hofmann, M., and Linnemann, U., 2015. Palaeomagnetic and geochronological data from Late Mesoproterozoic redbed sedimentary rocks on the western margin of Kalahari craton. *Geological Society, London, Special Publications*, v. 424, doi:10.1144/SP424.4.
- Kean, W., Williams, I., and Feeney, J., 1997. Magnetism of the Keweenawan age Chengwatana lava flows, northwest Wisconsin. *Geophysical Research Letters*, v. 24, p. 1523–1526, doi:10.1029/97gl00993.
- Kilian, T. M., Bleeker, W., Chamberlain, K., Evans, D. A. D., and Cousens, B., 2015. Palaeomagnetism, geochronology and geochemistry of the Palaeoproterozoic Rabbit Creek and Powder River dyke swarms: implications for Wyoming in supercraton Superia. *Geological Society, London, Special Publications*, v. 424, p. 15–45, doi:10.1144/sp424.7.
- Kilian, T. M., Chamberlain, K. R., Evans, D. A., Bleeker, W., and Cousens, B. L., 2016. Wyoming on the run—Toward final Paleoproterozoic assembly of Laurentia. *Geology*, v. 44, p. 863–866, doi:10.1130/g38042.1.
- Korenaga, J., 2013. Initiation and evolution of plate tectonics on Earth: Theories and observations. *Annual Review of Earth and Planetary Sciences*, v. 41, p. 117–151, doi:10.1146/annurev-earth-050212-124208.
- Kulakov, E. V., Smirnov, A. V., and Diehl, J. F., 2013. Paleomagnetism of ~1.09 Ga Lake Shore Traps (Keweenaw Peninsula, Michigan): new results and implications. *Canadian Journal of Earth Sciences*, v. 50, p. 1085–1096, doi:10.1139/cjes-2013-0003.
- Levy, M. and Christie-Blick, N., 1991. Tectonic subsidence of the early Paleozoic passive continental margin in eastern California and southern Nevada. *Geological Society of America Bulletin*, v. 103, p. 1590–1606, doi:10.1130/0016-7606(1991)103<1590:tsotep>2.3.co;2.
- Li, Z.-X., Evans, D. A. D., and Halverson, G., 2013. Neoproterozoic glaciations in a revised global palaeogeography from the breakup of Rodinia to the assembly of Gondwanaland. *Sedimentary Geology*, v. 294, p. 219–232, doi:10.1016/j.sedgeo.2013.05.016.
- Li, Z. X. et al., 2008. Assembly, configuration, and break-up history of Rodinia: A synthesis. *Precambrian Research*, v. 160, p. 179–210, doi:10.1016/j.precamres.2007.04.021.
- Loewy, S. L., Connelly, J. N., Dalziel, I. W., and Gower, C. F., 2003. Eastern Laurentia in Rodinia: constraints from whole-rock Pb and U/Pb geochronology. *Tectonophysics*, v. 375, p. 169–197, doi:10.1016/s0040-1951(03)00338-x.
- Lydon, J. W., 2004. Synopsis of the Belt-Purcell Basin. *Geological Survey of Canada Mineral Resources Division*, p. 1–27.
- Macdonald, F., Halverson, G., Strauss, J., Smith, E., Cox, G., Sperling, E., and Roots, C., 2012. Early Neoproterozoic basin formation in Yukon, Canada: Implications for the make-up and break-up of Rodinia. *Geoscience Canada*, v. 39, p. 77–99.
- Macdonald, F. A., Prave, A. R., Petterson, R., Smith, E. F., Pruss, S. B., Oates, K., Waechter, F., Trotzuk, D., and Fallick, A. E., 2013. The Laurentian record of Neoproterozoic glaciation, tectonism, and eukaryotic evolution in Death Valley, California. *Geological Society of America Bulletin*, v. 125, p. 1203–1223, doi:10.1130/B30789.1.

- Macdonald, F. A., Schmitz, M. D., Crowley, J. L., Roots, C. F., Jones, D. S., Maloof, A. C., Strauss, J. V., Cohen, P. A., Johnston, D. T., and Schrag, D. P., 2010. Calibrating the Cryogenian. *Science*, v. 327, p. 1241–1243, doi:10.1126/science.1183325.
- Macouin, M., Valet, J. P., Besse, J., and Ernst, R. E., 2006. Absolute paleointensity at 1.27 Ga from the Mackenzie dyke swarm (Canada). *Geochem. Geophys. Geosyst.*, v. 7, p. 10.1029/2005GC000,960.
- Maloof, A., Halverson, G., Kirschvink, J., Schrag, D., Weiss, B., and Hoffman, P., 2006. Combined paleomagnetic, isotopic and stratigraphic evidence for true polar wander from the Neoproterozoic Akademikerbreen Group, Svalbard, Norway. *Geological Society of America Bulletin*, v. 118, p. 1099–1124, doi:10.1130/B25892.1.
- Marcussen, C. and Abrahamsen, N., 1983. Palaeomagnetism of the Proterozoic Zig-Zag Dal Basalt and the Midsommersø Dolerites, eastern North Greenland. *Geophysical Journal International*, v. 73, p. 367–387, doi:10.1111/j.1365-246x.1983.tb03321.x.
- McCausland, P. J. A., Hankard, F., Van der Voo, R., and Hall, C. M., 2011. Ediacaran paleogeography of Laurentia: Paleomagnetism and 40Ar-39Ar geochronology of the 583 Ma Baie des Moutons syenite, Quebec. *Precambrian Research*, v. 187, p. 58–78, doi:10.1016/j.precamres.2011.02.004.
- McCausland, P. J. A., Van der Voo, R., and Hall, C. M., 2007. Circum-Iapetus paleogeography of the Precambrian–Cambrian transition with a new paleomagnetic constraint from Laurentia. *Precambrian Research*, v. 156, p. 125–152, doi:10.1016/j.precamres.2007.03.004.
- McFarlane, C. R., 2015. A geochronological framework for sedimentation and Mesoproterozoic tectono-magmatic activity in lower Belt–Purcell rocks exposed west of Kimberley, British Columbia. *Canadian Journal of Earth Sciences*, v. 52, p. 444–465, doi:10.1139/cjes-2014-0215.
- McGlynn, J. C., Hanson, G. N., Irving, E., and Park, J. K., 1974. Paleomagnetism and age of Nonacho Group sandstones and associated Sparrow dikes, District of Mackenzie. *Canadian Journal of Earth Sciences*, v. 11, p. 30–42, doi:10.1139/e74-003.
- McLlland, J. M., Selleck, B. W., and Bickford, M., 2010. Review of the Proterozoic evolution of the Grenville Province, its Adirondack outlier, and the Mesoproterozoic inliers of the Appalachians. From Rodinia to Pangea: The Lithotectonic Record of the Appalachian Region, p. 21–49, doi:10.1130/2010.1206(02).
- McLlland, J. M., Selleck, B. W., and Bickford, M. E., 2013. Tectonic evolution of the Adirondack Mountains and Grenville Orogen inliers within the USA. *Geoscience Canada*, v. 40, p. 318–352, doi:10.12789/geocanj.2013.40.022.
- McMechan, M. E. and Price, R. A., 1982. Superimposed low-grade metamorphism in the Mount Fisher area, southeastern British Columbia—implications for the East Kootenay orogeny. *Canadian Journal of Earth Sciences*, v. 19, p. 476–489, doi:10.1139/e82-039.
- Medig, K., Turner, E., Thorkelson, D., and Rainbird, R., 2016. Rifting of Columbia to form a deep-water siliciclastic to carbonate succession: The Mesoproterozoic Pinguicula Group of northern Yukon, Canada. *Precambrian Research*, v. 278, p. 179–206, doi:10.1016/j.precamres.2016.03.021.
- Meert, J., der Voo, R. V., and Payne, T., 1994. Paleomagnetism of the Catoctin volcanic province: a new Vendian-Cambrian apparent polar wander path for North America. *Journal of Geophysical Research*, v. 99, p. 4625–4641, doi:10.1029/93JB01723.
- Meert, J. G. and Stuckey, W., 2002. Revisiting the paleomagnetism of the 1.476 Ga St. Francois Mountains igneous province, Missouri. *Tectonics*, v. 21, doi:10.1029/2000tc001265.
- Merdith, A. S., Collins, A. S., Williams, S. E., Pisarevsky, S., Foden, J. D., Archibald, D. B., Blades, M. L., Alessio, B. L., Armistead, S., Plavsa, D., and et al., 2017. A full-plate global reconstruction of the Neoproterozoic. *Gondwana Research*, v. 50, p. 84–134, doi:10.1016/j.gr.2017.04.001.
- Met Office, 2010 - 2015, Cartopy: a cartographic python library with a matplotlib interface. Exeter, Devon, URL <http://scitools.org.uk/cartopy>.
- Middleton, R. S., Borradaile, G. J., Baker, D., and Lucas, K., 2004. Proterozoic diabase sills of northern Ontario: Magnetic properties and history. *Journal of Geophysical Research: Solid Earth*, v. 109, doi:10.1029/2003jb002581.
- Mitchell, R. N., Bleeker, W., van Breemen, O., Lecheminant, T. N., Peng, P., Nilsson, M. K. M., and Evans, D. A. D., 2014. Plate tectonics before 2.0 Ga: Evidence from paleomagnetism of cratons within supercontinent Nuna. *American Journal of Science*, v. 314, p. 878–894, doi:10.2475/04.2014.03.
- Mitchell, R. N., Hoffman, P. F., and Evans, D. A. D., 2010. Coronation loop resurrected: Oscillatory apparent polar wander of Orosirian (2.05–1.8 Ga) paleomagnetic poles from Slave craton. *Precambrian Research*, v. 179, p. 121–134, doi:10.1016/j.precamres.2010.02.018.
- Mitchell, R. N., Kilian, T. M., and Evans, D. A. D., 2012. Supercontinent cycles and the calculation of absolute palaeolongitude in deep time. *Nature*, v. 482, p. 208–211, doi:10.1038/nature10800.
- Mosher, S., 1998. Tectonic evolution of the southern Laurentian Grenville orogenic belt. *Geological Society of America Bulletin*, v. 110, p. 1357–1375, doi:10.1130/0016-7606(1998)110<1357:TEOTSL>2.3.CO;2.
- Müller, R. D., Cannon, J., Qin, X., Watson, R. J., Gurnis, M., Williams, S., Pfaffelmoser, T., Seton, M., Russell, S. H. J., and Záhrovec, S., 2018. GPlates: Building a virtual earth through deep time. *Geochemistry, Geophysics, Geosystems*, v. 19, p. 2243–2261, doi:10.1029/2018gc007584.
- Murthy, G., Gower, C., Tubett, M., and Patzold, R., 1992. Paleomagnetism of Eocambrian Long Range dykes and Double Mer Formation from Labrador, Canada. *Canadian Journal of Earth Sciences*, v. 29, p. 1224–1234, doi:10.1139/e92-098.
- Murthy, G. S., 1978. Paleomagnetic results from the Nain anorthosite and their tectonic implications. *Canadian Journal of Earth Sciences*, v. 15, p. 516–525, doi:10.1139/e78-058.
- Nesheim, T. O., Vervoort, J. D., McClelland, W. C., Gilotti, J. A., and Lang, H. M., 2012. Mesoproterozoic syntectonic garnet within Belt Supergroup metamorphic tectonites: Evidence of Grenville-age metamorphism and deformation along northwest Laurentia. *Lithos*, v. 134–135, p. 91–107, doi:10.1016/j.lithos.2011.12.008.
- Nimmo, F. and Stevenson, D. J., 2000. Influence of early plate tectonics on the thermal evolution and magnetic field of Mars. *Journal of Geophysical Research: Planets*, v. 105, p. 11,969–11,979, doi:10.1029/1999je001216.
- O'Neill, C., Lenardic, A., and Condie, K. C., 2013. Earth's punctuated tectonic evolution: cause and effect. *Geological Society, London, Special Publications*, v. 389, p. 17–40, doi:10.1144/sp389.4.
- Palin, R. M. and White, R. W., 2015. Emergence of blueschists on Earth linked to secular changes in oceanic crust composition. *Nature Geoscience*, v. 9, p. 60–64, doi:10.1038/ngeo2605.
- Palmer, H., 1970. Paleomagnetism and correlation of some Middle Keweenawan rocks, Lake Superior. *Canadian Journal of Earth Science*, v. 7, p. 1410–1436, doi:10.1139/e70-136.
- Palmer, H. C., Merz, B. A., and Hayatsu, A., 1977. The Sudbury dikes of the Grenville Front region: paleomagnetism, petrochemistry, and

- K–Ar age studies. Canadian Journal of Earth Sciences, v. 14, p. 1867–1887, doi:10.1139/e77-158.
- Park, J. K., Irving, E., and Donaldson, J. A., 1973. Paleomagnetism of the Precambrian Dubawnt Group. Geological Society of America Bulletin, v. 84, p. 859–870, doi:10.1130/0016-7606(1973)84<859:potpdg>2.0.co;2.
- Park, Y., Swanson-Hysell, N., Macdonald, F., and Lisiecki, L., 2020. Evaluating the relationship between the area and latitude of large igneous provinces and earth's long-term climate state. EarthArXiv, doi:10.31223/osf.io/p9ndf.
- Pehrsson, S. J., Eglington, B. M., Evans, D. A. D., Huston, D., and Reddy, S. M., 2015. Metallogeny and its link to orogenic style during the Nuna supercontinent cycle. Geological Society, London, Special Publications, v. 424, p. 83–94, doi:10.1144/SP424.5.
- Pérez, F. and Granger, B. E., 2007. IPython: a system for interactive scientific computing. Computing in Science and Engineering, v. 9, p. 21–29, doi:10.1109/MCSE.2007.53.
- Pesonen, L. J., 1979. Paleomagnetism of late Precambrian Keweenawan igneous and baked contact rocks from Thunder Bay district, northern Lake Superior. Bulletin of the Geological Society of Finland, v. 51, p. 27–44.
- Pesonen, L. J. and Halls, H., 1979. The paleomagnetism of Keweenawan dikes from Baraga and Marquette Counties, northern Michigan. Canadian Journal of Earth Science, v. 16, p. 2136–2149, doi:10.1139/e79-201.
- Piispa, E. J., Smirnov, A. V., Pesonen, L. J., and Mitchell, R. H., 2018. Paleomagnetism and geochemistry of 1144-Ma lamprophyre dikes, Northwestern Ontario: Implications for the North American polar wander and plate velocities. Journal of Geophysical Research: Solid Earth, v. 123, p. 6195–6214, doi:10.1029/2018jb015992.
- Piper, J., 1992. The palaeomagnetism of major (Middle Proterozoic) igneous complexes, South Greenland and the Gardar apparent polar wander track. Precambrian Research, v. 54, p. 153 – 172, doi:10.1016/0301-9268(92)90068-Y.
- Piper, J. and Stearn, J., 1977. Palaeomagnetism of the dyke swarms of the Gardar Igneous Province, south Greenland. Physics of the Earth and Planetary Interiors, v. 14, p. 345–358, doi:10.1016/0031-9201(77)90167-4.
- Piper, J. D. A., 1977. Palaeomagnetism of the giant dykes of Tugtutoq and Narssaq Gabbro, Gardar Igneous Province, South Greenland. Bull. Geol. Soc. Den., v. 26, p. 85–94.
- Pisarevsky, S. A., Elming, S.-Å., Pesonen, L. J., and Li, Z.-X., 2014. Mesoproterozoic paleogeography: Supercontinent and beyond. Precambrian Research, v. 244, p. 207–225, doi:10.1016/j.precamres.2013.05.014.
- Pisarevsky, S. A., Komissarova, R. A., and Khramov, A. N., 2001. Reply to comment by J.G. Meert and R. Van der Voo on 'New palaeomagnetic result from Vendian red sediments in Cisbaikalia and the problem of the relationship of Siberia and Laurentia in the Vendian'. Geophysical Journal International, v. 146, p. 871–873, doi:10.1046/j.0956-540x.2001.01475.x.
- Pratt, B. R., 2001. Oceanography, bathymetry and syndepositional tectonics of a Precambrian intracratonic basin: integrating sediments, storms, earthquakes and tsunamis in the Belt Supergroup (Helena Formation, ca. 1.45Ga), western North America. Sedimentary Geology, v. 141-142, p. 371–394, doi:10.1016/s0037-0738(01)00083-5.
- Pratt, B. R. and Ponce, J. J., 2019. Sedimentation, earthquakes, and tsunamis in a shallow, muddy epeiric sea: Grinnell Formation (Belt Supergroup, ca. 1.45 Ga), western North America. GSA Bulletin, v. 131, p. 1411–1439, doi:10.1130/b35012.1.
- Prince, J. K. G., 2014. Sequence stratigraphic, lithostratigraphic and stable isotopic analysis of the Minto Inlet Formation and Kilian Formation of the Shaler Supergroup, Northwest Territories. Master's thesis, Carleton University.
- Pullaiah, G. and Irving, E., 1975. Paleomagnetism of the contact aureole and late dikes of the Otto stock, Ontario, and its application to early Proterozoic apparent polar wandering. Canadian Journal of Earth Sciences, v. 12, p. 1609–1618, doi:10.1139/e75-143.
- Redden, J., Peterman, Z., Zartman, R., and De-Witt, E., 1990. U-Th-Pb geochronology and preliminary interpretation of Precambrian tectonic events in the Black Hills, South Dakota. In *The Early Proterozoic Trans-Hudson Orogen*, Geological Association of Canada Special Paper 37, p. 229–251.
- RiouxB, M., Bowring, S., Dudás, F., and Hanson, R., 2010. Characterizing the U–Pb systematics of baddeleyite through chemical abrasion: application of multi-step digestion methods to baddeleyite geochronology. Contributions to Mineralogy and Petrology, v. 160, p. 777–801, doi:10.1007/s00410-010-0507-1.
- Rivers, T., 2008. Assembly and preservation of lower, mid, and upper orogenic crust in the Grenville Province—implications for the evolution of large hot long-duration orogens. Precambrian Research, v. 167, p. 237–259, doi:10.1016/j.precamres.2008.08.005.
- Robert, B., Besse, J., Blein, O., Greff-Lefftz, M., Baudin, T., Lopes, F., Meslouh, S., and Belbadaoui, M., 2017. Constraints on the Ediacaran inertial interchange true polar wander hypothesis: A new paleomagnetic study in Morocco (West African Craton). Precambrian Research, v. 295, p. 90–116, doi:10.1016/j.precamres.2017.04.010.
- Robert, B., Domeier, M., and Jakob, J., 2020. Iapetan Oceans: An analog of Tethys?. Geology, doi:10.1130/g47513.1.
- Robertson, W. and Fahrig, W., 1971. The great Logan Loop - the polar wandering path from Canadian shield rocks during the Neohelikian era. Canadian Journal of Earth Science, v. 8, p. 1355–1372, doi:10.1139/e71-125.
- Roest, W. R. and Srivastava, S. P., 1989. Sea-floor spreading in the Labrador Sea: A new reconstruction. Geology, v. 17, p. 1000–1003, doi:10.1130/0091-7613(1989)017<1000:sfsitl>2.3.co;2.
- Rooney, A. D., Austermann, J., Smith, E. F., Li, Y., Selby, D., Dehler, C. M., Schmitz, M. D., Karlstrom, K. E., and Macdonald, F. A., 2017. Coupled Re-Os and U-Pb geochronology of the Tonian Chuar Group, Grand Canyon. GSA Bulletin, v. 130, p. 1085–1098, doi:10.1130/b31768.1.
- Ross, G. M., 1991. Tectonic setting of the Windermere Supergroup revisited. Geology, v. 19, p. 1125–1128, doi:10.1130/0091-7613(1991)019<1125:tsotws>2.3.co;2.
- Schmidt, P. W., 1980. Paleomagnetism of igneous rocks from the Belcher Islands, Northwest Territories, Canada. Canadian Journal of Earth Sciences, v. 17, p. 807–822, doi:10.1139/e80-081.
- Schulz, K. J. and Cannon, W. F., 2007. The Penokean orogeny in the Lake Superior region. Precambrian Research, v. 157, p. 4–25, doi:10.1016/j.precamres.2007.02.022.
- Schwarz, E. J., Clark, K. R., and Fujiwara, Y., 1982. Paleomagnetism of the Sutton Lake Proterozoic inlier, Ontario, Canada. Canadian Journal of Earth Sciences, v. 19, p. 1330–1332, doi:10.1139/e82-114.
- Sears, J. W., Chamberlain, K. R., and Buckley, S. N., 1998. Structural and U-Pb geochronological evidence for 1.47 Ga rifting in the Belt basin, western Montana. Canadian Journal of Earth Sciences, v. 35, p. 467–475, doi:10.1139/e97-121.
- Selkin, P. A., Gee, J. S., Meurer, W. P., and Hemming, S. R., 2008. Paleointensity record from the 2.7 Ga Stillwater Complex, Montana. Geochem. Geophys. Geosyst., v. 9, p. 10.1029/2008GC001,950.

- Silver, P. G. and Behn, M. D., 2008. Intermittent plate tectonics?. *Science*, v. 319, p. 85–88, doi:10.1126/science.1148397.
- Skipton, D. R., St-Onge, M. R., Schneider, D. A., and McFarlane, C. R. M., 2016. Tectono-thermal evolution of the middle crust in the Trans-Hudson Orogen, Baffin Island, Canada: Evidence from petrology and monazite geochronology of sillimanite-bearing migmatites. *Journal of Petrology*, v. 57, p. 1437–1462, doi:10.1093/petrology/egw046.
- Slagstad, T., Culshaw, N. G., Daly, J. S., and Jamieson, R. A., 2009. Western Grenville Province holds key to midcontinental Granite-Rhyolite Province enigma. *Terra Nova*, v. 21, p. 181–187, doi:10.1111/j.1365-3121.2009.00871.x.
- Smith, E. F., Macdonald, F. A., Crowley, J. L., Hodgin, E. B., and Schrag, D. P., 2015. Tectonostratigraphic evolution of the c. 780–730 Ma Beck Spring Dolomite: Basin Formation in the core of Rodinia. Geological Society, London, Special Publications, v. 424, doi:10.1144/SP424.6.
- Spencer, C. J., Thomas, R. J., Roberts, N. M., Cawood, P. A., Millar, I., and Tapster, S., 2015. Crustal growth during island arc accretion and transcurrent deformation, natal metamorphic province, south africa: New isotopic constraints. *Precambrian Research*, v. 265, p. 203–217, doi:10.1016/j.precamres.2015.05.011.
- St-Onge, M. R., Van Gool, J. A. M., Garde, A. A., and Scott, D. J., 2009. Correlation of Archaean and Palaeoproterozoic units between northeastern Canada and western Greenland: constraining the pre-collisional upper plate accretionary history of the Trans-Hudson orogen. Geological Society, London, Special Publications, v. 318, p. 193–235, doi:10.1144/sp318.7.
- Stern, R. J. and Miller, N. R., 2018. Did the transition to plate tectonics cause Neoproterozoic Snowball Earth?. *Terra Nova*, v. 30, p. 87–94, doi:10.1111/ter.12321.
- Stern, R. J., Tsujimori, T., Harlow, G., and Groat, L. A., 2013. Plate tectonic gemstones. *Geology*, v. 41, p. 723–726, doi:10.1130/g34204.1.
- Swanson-Hysell, N. L., Burgess, S. D., Maloof, A. C., and Bowring, S. A., 2014a. Magmatic activity and plate motion during the latent stage of Midcontinent Rift development. *Geology*, v. 42, p. 475–478, doi:10.1130/G35271.1.
- Swanson-Hysell, N. L., Maloof, A. C., Condon, D. J., Jenkin, G. R. T., Alene, M., Tremblay, M. M., Tesema, T., Rooney, A. D., and Haileab, B., 2015. Stratigraphy and geochronology of the Tambien Group, Ethiopia: Evidence for globally synchronous carbon isotope change in the Neoproterozoic. *Geology*, doi:10.1130/G36347.1.
- Swanson-Hysell, N. L., Ramezani, J., Fairchild, L. M., and Rose, I. R., 2019. Failed rifting and fast drifting: Midcontinent Rift development, Laurentia's rapid motion and the driver of Grenvillian orogenesis. *GSA Bulletin*, v. 131, p. 913–940, doi:10.1130/b31944.1.
- Swanson-Hysell, N. L., Vaughan, A. A., Mustain, M. R., and Asp, K. E., 2014b. Confirmation of progressive plate motion during the Midcontinent Rift's early magmatic stage from the Osler Volcanic Group, Ontario, Canada. *Geochemistry Geophysics Geosystems*, v. 15, p. 2039–2047, doi:10.1002/2013GC005180.
- Symons, D. and Chiasson, A., 1991. Paleomagnetism of the Callander Complex and the Cambrian apparent polar wander path for North America. *Canadian Journal of Earth Science*, v. 1991, p. 355–363, doi:10.1139/e91-032.
- Symons, D., Symons, T., and Lewchuk, M., 2000. Paleomagnetism of the Deschambault pegmatites: Stillstand and hairpin at the end of the Paleoproterozoic Trans-Hudson Orogeny, Canada. *Physics and Chemistry of the Earth, Part A: Solid Earth and Geodesy*, v. 25, p. 479–487, doi:10.1016/s1464-1895(00)00074-0.
- Symons, D. T. A. and Mackay, C. D., 1999. Paleomagnetism of the Boot-Phantom pluton and the amalgamation of the juvenile domains in the Paleoproterozoic Trans-Hudson Orogen, Canada. In Sinha, A. K., ed., *Basement Tectonics 13*, Springer Netherlands, Dordrecht, p. 313–331, doi:10.1007/978-94-011-4800-9\_18.
- Tanczyk, E., Lapointe, P., Morris, W., and Schmidt, P., 1987. A paleomagnetic study of the layered mafic intrusions at Sept-Iles, Quebec. *Canadian Journal of Earth Science*, v. 24, p. 1431–1438, doi:10.1139/e87-135.
- Tauxe, L. and Kodama, K., 2009. Paleosecular variation models for ancient times: Clues from Keweenawan lava flows. *Physics of the Earth and Planetary Interiors*, v. 177, p. 31–45, doi:10.1016/j.pepi.2009.07.006.
- Tauxe, L., Shaar, R., Jonestrask, L., Swanson-Hysell, N., Minnett, R., Koppers, A., Constable, C., Jarboe, N., Gaastra, K., and Fairchild, L., 2016. PmagPy: Software package for paleomagnetic data analysis and a bridge to the Magnetics Information Consortium (MagIC) Database. *Geochemistry, Geophysics, Geosystems*, v. 17, p. 2450–2463, doi:10.1002/2016GC006307.
- Thallner, D., Biggin, A., and Halls, H. C., 2020. The Ediacaran Grenville dykes (SE Canada) reveal the weakest sustained palaeomagnetic field on record. *EarthArxiv*, doi:10.31223/osf.io/ksqhy.
- Thiessen, E. J., Gibson, H. D., Regis, D., Pehrsson, S. J., Ashley, K. T., and Smit, M. A., 2020. The distinct metamorphic stages and structural styles of the 1.94–1.86 Ga Snowbird Orogen, Northwest Territories, Canada. *Journal of Metamorphic Geology*, doi:10.1111/jmg.12556.
- Torsvik, T. H. and Cocks, L. R. M., 2017. Earth history and palaeogeography. Cambridge University Press, doi:10.1017/9781316225523.
- Torsvik, T. H., van der Voo, R., Doubrovine, P. V., Burke, K., Steinberger, B., Ashwal, L. D., Trønnes, R. G., Webb, S. J., and Bull, A. L., 2014. Deep mantle structure as a reference frame for movements in and on the Earth. *Proceedings of the National Academy of Sciences*, v. 111, p. 8735–8740, doi:10.1073/pnas.1318135111.
- Torsvik, T. H., Van der Voo, R., Preeden, U., Mac Niocaill, C., Steinberger, B., Doubrovine, P. V., van Hinsbergen, D. J. J., Domeier, M., Gaina, C., Tohver, E., Meert, J. G., McCausland, P. J. A., and Cocks, L. R. M., 2012. Phanerozoic polar wander, palaeogeography and dynamics. *Earth-Science Reviews*, v. 114, p. 325–368, doi:10.1016/j.earscirev.2012.06.007.
- Turner, E. C. and Bekker, A., 2016. Thick sulfate evaporite accumulations marking a mid-Neoproterozoic oxygenation event (Ten Stone Formation, Northwest Territories, Canada). *Geological Society of America Bulletin*, v. 128, p. 203–222, doi:10.1130/B31268.1.
- Veikkilainen, T., Pesonen, L., and Evans, D. A. D., 2014. PALEOMAGIA: A PHP/MYSQL database of the Precambrian paleomagnetic data. *Studia Geophysica et Geodaetica*, v. 58, p. 1–17, doi:10.1007/s11200-013-0382-0.
- Verbaas, J., Thorkelson, D. J., Milidragovic, D., Crowley, J. L., Foster, D., Daniel Gibson, H., and Marshall, D. D., 2018. Rifting of western Laurentia at 1.38 Ga: The Hart River sills of Yukon, Canada. *Lithos*, v. 316–317, p. 243–260, doi:10.1016/j.lithos.2018.06.018.
- Wang, C.-C., Jacobs, J., Elburg, M. A., Läufer, A., Thomas, R. J., and Elvevold, S., 2020. Grenville-age continental arc magmatism and crustal evolution in central Dronning Maud Land (East Antarctica): Zircon geochronological and Hf–O isotopic evidence. *Gondwana Research*, v. 82, p. 108–127, doi:10.1016/j.gr.2019.12.004.
- Warnock, A., Kodama, K., and Zeitler, P., 2000. Using thermochronometry and low-temperature demagnetization to accurately date Precambrian paleomagnetic poles. *Journal of Geophysical Research*, v. 105, p. 19,435–19,453, doi:10.1029/2000jb900114.

- Weil, A., Geissman, J., Heizler, M., and Van der Voo, R., 2003. Paleomagnetism of Middle Proterozoic mafic intrusions and Upper Proterozoic (Nankoweap) red beds from the Lower Grand Canyon Supergroup, Arizona. *Tectonophysics*, v. 375, p. 199–220, doi:10.1016/S0040-1951(03)00339-1.
- Weil, A. B., Geissman, J. W., and Ashby, J. M., 2006. A new paleomagnetic pole for the Neoproterozoic Uinta Mountain supergroup, Central Rocky Mountain States, USA. *Precambrian Research*, v. 147, p. 234–259, doi:10.1016/j.precamres.2006.01.017.
- Weil, A. B., Geissman, J. W., and Voo, R. V. d., 2004. Paleomagnetism of the Neoproterozoic Chuar Group, Grand Canyon Supergroup, Arizona: implications for Laurentia's Neoproterozoic APWP and Rodinia break-up. *Precambrian Research*, v. 129, p. 71–92, doi:10.1016/j.precamres.2003.09.016.
- Weller, O. M. and St-Onge, M. R., 2017. Record of modern-style plate tectonics in the Palaeoproterozoic Trans-Hudson orogen. *Nature Geoscience*, v. 10, p. 305–311, doi:10.1038/ngeo2904.
- White, B., 1984. Stromatolites and associated facies in shallowing-upward cycles from the middle Proterozoic Altyn Formation of Glacier National Park, Montana. *Precambrian Research*, v. 24, p. 1–26, doi:10.1016/0301-9268(84)90067-6.
- Whitmeyer, S. and Karlstrom, K., 2007. Tectonic model for the Proterozoic growth of North America. *Geosphere*, v. 3, p. 220–259, doi:10.1130/GES00055.1.
- Winston, D., 2007. Revised stratigraphy and depositional history of the Helena and Wallace Formations, mid-Proterozoic Piegan Group, Belt Supergroup, Montana and Idaho, U.S.A.. In *Proterozoic Geology of Western North America and Siberia*, SEPM (Society for Sedimentary Geology), p. 65–100, doi:10.2110/pec.07.86.0065.
- Witkosky, R. and Wernicke, B. P., 2018. Subsidence history of the Ediacaran Johnnie Formation and related strata of southwest Laurentia: Implications for the age and duration of the Shuram isotopic excursion and animal evolution. *Geosphere*, v. 14, p. 2245–2276, doi:10.1130/ges01678.1.
- Yonkee, W., Dehler, C., Link, P., Balgord, E., Keeley, J., Hayes, D., Wells, M., Fanning, C., and Johnston, S., 2014. Tectono-stratigraphic framework of Neoproterozoic to Cambrian strata, west-central U.S.: Protracted rifting, glaciation, and evolution of the North American Cordilleran margin. *Earth-Science Reviews*, v. 136, p. 59–95, doi:10.1016/j.earscirev.2014.05.004.
- Zhang, S., Chang, H., L. Zhao, Ding, J., Xian, H., Li, H., Wu, H., and Yang, T., 2021. The Precambrian drift history and paleogeography of the Chinese cratons. In Pesonen, L. J., Evans, D. A. D., Elming, S. Å., Salminen, J. M., and Veikkolainen, T., eds., *Ancient Supercontinents and the Paleogeography of the Earth*, Elsevier.
- Zhang, S., Li, Z.-X., Evans, D. A. D., Wu, H., Li, H., and Dong, J., 2012. Pre-Rodinia supercontinent Nuna shaping up: A global synthesis with new paleomagnetic results from North China. *Earth and Planetary Science Letters*, v. 353–354, p. 145–155, doi:10.1016/j.epsl.2012.07.034.
- Zhao, H., Zhang, S., Ding, J., Chang, L., Ren, Q., Li, H., Yang, T., and Wu, H., 2019. New geochronologic and paleomagnetic results from early Neoproterozoic mafic sills and late Mesoproterozoic to early Neoproterozoic successions in the eastern North China Craton, and implications for the reconstruction of Rodinia. *GSA Bulletin*, v. 132, p. 739–766, doi:10.1130/b35198.1.

**Table 2:** Compilation of paleomagnetic poles from Laurentia

terrane	unit name	Nordic rating	site lon (°)	site lat (°)	plon (°)	plat (°)	A <sub>95</sub> (°)	age (Ma)	pole reference
Laurentia-Wyoming	Stillwater Complex - C2	A	249.2	45.2	335.8	-83.6	4.0	2705 <sup>+4</sup> <sub>-4</sub>	Selkin et al. (2008)
Laurentia-Superior(East)	Otto Stock dykes and aureole	B	279.9	48.0	227.0	69.0	4.8	2676 <sup>+5</sup> <sub>-5</sub>	Pullaiah and Irving (1975)
Laurentia-Slave	Defeat Suite	B	245.5	62.5	64.0	-1.0	15.0	2625 <sup>+5</sup> <sub>-5</sub>	Mitchell et al. (2014)
Laurentia-Superior(East)	Ptarmigan-Mistassini dykes	B	287.0	54.0	213.0	-45.3	13.8	2505 <sup>+5</sup> <sub>-2</sub>	Evans and Halls (2010)
Laurentia-Superior(East)	Matachewan dykes R	A	278.0	48.0	238.3	-44.1	1.6	2466 <sup>+23</sup> <sub>-23</sub>	Evans and Halls (2010)
Laurentia-Superior(East)	Matachewan dykes N	A	278.0	48.0	239.5	-52.3	2.4	2446 <sup>+3</sup> <sub>-3</sub>	Evans and Halls (2010)
Laurentia-Slave	Malley dykes	A	249.8	64.2	310.0	-50.8	6.7	2231 <sup>+2</sup> <sub>-2</sub>	Buchan et al. (2012)
Laurentia-Superior(East)	Senneterre dykes	A	283.0	49.0	284.3	-15.3	5.5	2218 <sup>+6</sup> <sub>-6</sub>	Buchan et al. (1993)
Laurentia-Superior(East)	Nipissing NI sills	A	279.0	47.0	272.0	-17.0	10.0	2217 <sup>+4</sup> <sub>-4</sub>	Buchan et al. (2000)
Laurentia-Slave	Dogrib dykes	A	245.5	62.5	315.0	-31.0	7.0	2193 <sup>+2</sup> <sub>-2</sub>	Mitchell et al. (2014)
Laurentia-Superior(East)	Biscotasing dykes	A	280.0	48.0	223.9	26.0	7.0	2170 <sup>+3</sup> <sub>-3</sub>	Evans and Halls (2010)
Laurentia-Wyoming	Rabbit Creek, Powder River and South Path Dykes	A	252.8	43.9	339.2	65.5	7.6	2160 <sup>+11</sup> <sub>-8</sub>	Kilian et al. (2015)
Laurentia-Slave	Indin dykes	A	245.6	62.5	256.0	-36.0	7.0	2126 <sup>+3</sup> <sub>-18</sub>	Buchan et al. (2016)
Laurentia-Superior(West)	Marathon dykes N	A	275.0	49.0	198.2	45.4	7.7	2124 <sup>+3</sup> <sub>-3</sub>	Halls et al. (2008)
Laurentia-Superior(West)	Marathon dykes R	A	275.0	49.0	182.2	55.1	7.5	2104 <sup>+3</sup> <sub>-3</sub>	Halls et al. (2008)
Laurentia-Superior(West)	Cauchon Lake dykes	A	263.0	56.0	180.9	53.8	7.7	2091 <sup>+2</sup> <sub>-2</sub>	Evans and Halls (2010)
Laurentia-Superior(West)	Fort Frances dykes	A	266.0	48.0	184.6	42.8	6.1	2077 <sup>+5</sup> <sub>-5</sub>	Evans and Halls (2010)
Laurentia-Superior(East)	Lac Esprit dykes	A	282.0	53.0	170.5	62.0	6.4	2069 <sup>+1</sup> <sub>-1</sub>	Evans and Halls (2010)
Laurentia-Greenland-Nain	Kangamiut Dykes	B	307.0	66.0	273.8	17.1	2.7	2042 <sup>+12</sup> <sub>-12</sub>	Fahrig and Bridgwater (1976)
Laurentia-Slave	Lac de Gras dykes	A	249.6	64.4	267.9	11.8	7.1	2026 <sup>+5</sup> <sub>-5</sub>	Buchan et al. (2009)
Laurentia-Superior(East)	Minto dykes	A	285.0	57.0	171.5	38.7	13.1	1998 <sup>+2</sup> <sub>-2</sub>	Evans and Halls (2010)
Laurentia-Slave	Rifle Formation	B	252.9	65.9	341.0	14.0	7.7	1963 <sup>+6</sup> <sub>-6</sub>	Evans and Hoye (1981)
Laurentia-Rae	Clearwater Anorthosite	B	251.6	57.1	311.8	6.5	2.9	1917 <sup>+7</sup> <sub>-7</sub>	Halls and Hanes (1999)
Laurentia-Wyoming	Sourdough mafic dike swarm	A	-108.3	44.7	292.0	49.2	8.1	1899 <sup>+5</sup> <sub>-5</sub>	Kilian et al. (2016)
Laurentia-Slave	Ghost Dike Swarm	A	244.6	62.6	286.0	-2.0	6.0	1887 <sup>+5</sup> <sub>-9</sub>	Buchan et al. (2016)
Laurentia-Slave	Mean Seaton/Akaitcho/Mara	B	250.0	65.0	260.0	-6.0	4.0	1885 <sup>+5</sup> <sub>-5</sub>	Mitchell et al. (2010)
Laurentia-Slave	Mean Kahocheilla, Peacock Hills	B	250.0	65.0	285.0	-12.0	7.0	1882 <sup>+4</sup> <sub>-4</sub>	Mitchell et al. (2010)
Laurentia-Superior(West)	Molson (B+C2) dykes	A	262.0	55.0	218.0	28.9	3.8	1879 <sup>+6</sup> <sub>-6</sub>	Evans and Halls (2010)
Laurentia-Slave	Douglas Peninsula Formation, Pethci Group	B	249.7	62.8	258.0	-18.0	14.2	1876 <sup>+10</sup> <sub>-10</sub>	Irving and McGlynn (1979)
Laurentia-Slave	Takiyuak Formation	B	246.9	66.1	249.0	-13.0	8.0	1876 <sup>+10</sup> <sub>-10</sub>	Irving and McGlynn (1979)
Laurentia-Superior	Haig/Flaherty/Sutton Mean	B	279.0	56.0	245.8	1.0	3.9	1870 <sup>+1</sup> <sub>-1</sub>	Nordic workshop calculation based on data of Schmidt (1980); Schwarz et al. (1982)
Laurentia-Slave	Pearson A/Peninsular/Kilohigok sills	A	250.0	65.0	269.0	-22.0	6.0	1870 <sup>+4</sup> <sub>-4</sub>	Mitchell et al. (2010)
Laurentia-Trans-Hudson orogen	Boot-Phantom Pluton	B	258.1	54.7	275.4	62.4	7.9	1838 <sup>+1</sup> <sub>-1</sub>	Symons and Mackay (1999)
Laurentia-Rae	Sparrow Dykes	B	250.2	61.6	291.0	12.0	7.9	1827 <sup>+4</sup> <sub>-4</sub>	McGlynn et al. (1974)
Laurentia-Rae	Martin Formation	A	251.4	59.6	288.0	-9.0	8.5	1818 <sup>+4</sup> <sub>-4</sub>	Evans and Bingham (1973)
Laurentia	Dubawnt Group	B	265.6	64.1	277.0	7.0	8.0	1785 <sup>+35</sup> <sub>-35</sub>	Park et al. (1973)
Laurentia-Trans-Hudson orogen	Deschambault Pegmatites	B	256.7	54.9	276.0	67.5	7.7	1766 <sup>+5</sup> <sub>-5</sub>	Symons et al. (2000)

Continued on next page

terrane	unit name	Nordic rating	site lon (°)	site lat (°)	plon (°)	plat (°)	A <sub>95</sub> (°)	age (Ma)	pole reference
Laurentia-Trans-Hudson orogen	Jan Lake Granite	B	257.2	54.9	264.3	24.3	16.9	1758 <sup>+1</sup> <sub>-1</sub>	Gala et al. (1995)
Laurentia	Cleaver Dykes	A	242.0	67.5	276.7	19.4	6.1	1741 <sup>+5</sup> <sub>-5</sub>	Irving (2004)
Laurentia-Greenland	Melville Bugt diabase dykes	B	303.0	74.6	273.8	5.0	8.7	1633 <sup>+5</sup> <sub>-5</sub>	Halls et al. (2011)
Laurentia	Western Channel Diabase	A	242.2	66.4	245.0	9.0	6.6	1590 <sup>+3</sup> <sub>-3</sub>	Irving and Park (1972)
Laurentia	St.Francois Mountains Acidic Rocks	A	269.5	37.5	219.0	-13.2	6.1	1476 <sup>+16</sup> <sub>-16</sub>	Meert and Stuckey (2002)
Laurentia	Michikamau Intrusion	A	296.0	54.5	217.5	-1.5	4.7	1460 <sup>+5</sup> <sub>-5</sub>	Emslie et al. (1976)
Laurentia	Spokane Formation	A	246.8	48.2	215.5	-24.8	4.7	1458 <sup>+13</sup> <sub>-13</sub>	Elston et al. (2002)
Laurentia	Snowslip Formation	A	245.9	47.9	210.2	-24.9	3.5	1450 <sup>+14</sup> <sub>-14</sub>	Elston et al. (2002)
Laurentia	Tobacco Root dykes	B	247.6	47.4	216.1	8.7	10.5	1448 <sup>+40</sup> <sub>-49</sub>	Harlan et al. (2008)
Laurentia	Purcell Lava	A	245.1	49.4	215.6	-23.6	4.8	1443 <sup>+7</sup> <sub>-7</sub>	Elston et al. (2002)
Laurentia	Rocky Mountain intrusions	B	253.8	40.3	217.4	-11.9	9.7	1430 <sup>+15</sup> <sub>-15</sub>	Nordic workshop calculation based on data of Harlan et al. (1994); Harlan and Geissman (1998)
Laurentia	Mistastin Pluton	B	296.3	55.6	201.5	-1.0	7.6	1425 <sup>+25</sup> <sub>-25</sub>	Fahrig and Jones (1976)
Laurentia	McNamara Formation	A	246.4	46.9	208.3	-13.5	6.7	1401 <sup>+6</sup> <sub>-6</sub>	Elston et al. (2002)
Laurentia	Pilcher, Garnet Range and Libby Formations	A	246.4	46.7	215.3	-19.2	7.7	1385 <sup>+23</sup> <sub>-23</sub>	Elston et al. (2002)
Laurentia-Greenland	Zig-Zag Dal Basalts	B	334.8	81.2	242.8	12.0	3.8	1382 <sup>+2</sup> <sub>-2</sub>	Marcussen and Abrahamsen (1983)
Laurentia-Greenland	Midsommersoe Dolerite	B	333.4	81.6	242.0	6.9	5.1	1382 <sup>+2</sup> <sub>-2</sub>	Marcussen and Abrahamsen (1983)
Laurentia-Greenland	Victoria Fjord dolerite dykes	B	315.3	81.5	231.7	10.3	4.3	1382 <sup>+2</sup> <sub>-2</sub>	Abrahamsen and Van Der Voo (1987)
Laurentia	Nain Anorthosite	B	298.2	56.5	206.7	11.7	2.2	1305 <sup>+15</sup> <sub>-15</sub>	Murthy (1978)
Laurentia-Greenland	North Qoroq intrusives	B	314.6	61.1	202.6	13.2	8.3	1275 <sup>+1</sup> <sub>-1</sub>	Piper (1992)
Laurentia-Greenland	Kungnai Ring Dyke	B	311.7	61.2	198.7	3.4	3.2	1275 <sup>+2</sup> <sub>-2</sub>	Piper and Stearn (1977)
Laurentia	Mackenzie dykes grand mean	A	250.0	65.0	190.0	4.0	5.0	1267 <sup>+2</sup> <sub>-2</sub>	Buchan et al. (2000)
Laurentia-Greenland	West Gardar Dolerite Dykes	B	311.7	61.2	201.7	8.7	6.6	1244 <sup>+8</sup> <sub>-8</sub>	Piper and Stearn (1977)
Laurentia-Greenland	West Gardar Lamprophyre Dykes	B	311.7	61.2	206.4	3.2	7.2	1238 <sup>+11</sup> <sub>-11</sub>	Piper and Stearn (1977)
Laurentia	Sudbury Dykes Combined	A	278.6	46.3	192.8	-2.5	2.5	1237 <sup>+5</sup> <sub>-5</sub>	Palmer et al. (1977)
Laurentia-Scotland	Stoer Group	B	354.5	58.0	238.4	37.2	7.7	1199 <sup>+70</sup> <sub>-70</sub>	Nordic workshop calculation
Laurentia-Greenland	Narsaq Gabbro	B	313.8	60.9	225.4	31.6	9.7	1184 <sup>+5</sup> <sub>-5</sub>	Piper (1977)
Laurentia-Greenland	Hviddal Giant Dyke	B	313.7	60.9	215.3	33.2	9.6	1184 <sup>+5</sup> <sub>-5</sub>	Piper (1977)
Laurentia-Greenland	South Qoroq Intr.	A	314.6	61.1	215.9	41.8	13.1	1163 <sup>+2</sup> <sub>-2</sub>	Piper (1992)
Laurentia-Greenland	Giant Gabbro Dykes	B	313.7	60.9	226.1	42.3	9.4	1163 <sup>+2</sup> <sub>-2</sub>	Piper (1977)
Laurentia-Greenland	NE-SW Trending dykes	B	314.6	61.1	230.8	33.4	5.7	1160 <sup>+5</sup> <sub>-5</sub>	Piper (1992)
Laurentia	Ontario lamprophyre dykes	NR	273.3	48.8	223.3	58.0	9.2	1143 <sup>+10</sup> <sub>-10</sub>	Pisipa et al. (2018)
Laurentia	Abitibi Dykes	A	279.0	48.0	215.5	48.8	14.1	1141 <sup>+2</sup> <sub>-2</sub>	Ernst and Buchan (1993)
Laurentia	Nipigon sills and lavas	A	270.9	49.1	217.8	47.2	4.0	1109 <sup>+2</sup> <sub>-2</sub>	Nordic workshop calculation based on data of Palmer (1970); Robertson and Fahrig (1971); Pesonen (1979); Pesonen and Halls (1979); Middleton et al. (2004); Borradale and Middleton (2006)
Laurentia	Lowermost Mamainse Point volcanics -R1	A	275.3	47.1	227.0	49.5	5.3	1109 <sup>+2</sup> <sub>-3</sub>	Swanson-Hysell et al. (2014a)
Laurentia	Lower Osler volcanics -R	A	272.3	48.8	218.6	40.9	4.8	1108 <sup>+3</sup> <sub>-3</sub>	Swanson-Hysell et al. (2014b)
Laurentia	Middle Osler volcanics - R	A	272.4	48.8	211.3	42.7	8.2	1107 <sup>+4</sup> <sub>-4</sub>	Swanson-Hysell et al. (2014b)

Continued on next page

terrane	unit name	Nordic rating	site lon (°)	site lat (°)	plon (°)	plat (°)	A <sub>95</sub> (°)	age (Ma)	pole reference
Laurentia	Upper Osler volcanics -R	A	272.4	48.7	203.4	42.3	3.7	1105 <sup>+1</sup> <sub>-1</sub>	Halls (1974); Swanson-Hysell et al. (2014b, 2019)
Laurentia	Lower Mamainse Point volcanics -R2	A	275.3	47.1	205.2	37.5	4.5	1105 <sup>+3</sup> <sub>-4</sub>	Swanson-Hysell et al. (2014a)
Laurentia	Mamainse Point volcanics -C (lower N, upper R)	A	275.3	47.1	189.7	36.1	4.9	1101 <sup>+1</sup> <sub>-1</sub>	Swanson-Hysell et al. (2014a)
Laurentia	North Shore lavas -N	A	268.7	46.3	181.7	31.1	2.1	1097 <sup>+3</sup> <sub>-3</sub>	Tauxe and Kodama (2009); Swanson-Hysell et al. (2019)
Laurentia	Portage Lake Volcanics	A	271.2	47.0	182.5	27.5	2.3	1095 <sup>+3</sup> <sub>-3</sub>	Books (1972); Hnat et al. (2006) as calculated in Swanson-Hysell et al. (2019)
Laurentia	Chengwatana Volcanics	B	267.3	45.4	186.1	30.9	8.2	1095 <sup>+2</sup> <sub>-2</sub>	Kean et al. (1997)
Laurentia	Uppermost Mamainse Point volcanics -N	A	275.3	47.1	183.2	31.2	2.5	1094 <sup>+6</sup> <sub>-4</sub>	Swanson-Hysell et al. (2014a)
Laurentia	Cardenas Basalts and Intrusions	B	248.1	36.1	185.0	32.0	8.0	1091 <sup>+5</sup> <sub>-5</sub>	Weil et al. (2003)
Laurentia	Schroeder Lutsen Basalts	A	269.1	47.5	187.8	27.1	3.0	1090 <sup>+2</sup> <sub>-7</sub>	Fairchild et al. (2017)
Laurentia	Central Arizona diabases -N	A	249.2	33.7	175.3	15.7	7.0	1088 <sup>+11</sup> <sub>-11</sub>	Donadini et al. (2011)
Laurentia	Lake Shore Traps	A	271.9	47.6	186.4	23.1	4.0	1086 <sup>+1</sup> <sub>-1</sub>	Kulakov et al. (2013)
Laurentia	Michipicoten Island Formation	A	274.3	47.7	174.7	17.0	4.4	1084 <sup>+1</sup> <sub>-1</sub>	Fairchild et al. (2017)
Laurentia	Nonesuch Shale	B	271.5	47.0	178.1	7.6	5.5	1080 <sup>+4</sup> <sub>-10</sub>	Henry et al. (1977)
Laurentia	Freida Sandstone	B	271.5	47.0	179.0	2.2	4.2	1070 <sup>+14</sup> <sub>-10</sub>	Henry et al. (1977)
Laurentia	Haliburton Intrusions	B	281.4	45.0	141.9	-32.6	6.3	1015 <sup>+15</sup> <sub>-15</sub>	Warnock et al. (2000)
Laurentia-Scotland	Torridon Group	B	354.3	57.9	220.9	-17.7	7.1	925 <sup>+145</sup> <sub>-145</sub>	Nordic workshop calculation
Laurentia-Svalbard	Lower Grusdievbreen Formation	B	18.0	79.0	204.9	19.6	10.9	831 <sup>+20</sup> <sub>-20</sub>	Maloof et al. (2006)
Laurentia-Svalbard	Upper Grusdievbreen Formation	B	18.2	78.9	252.6	-1.1	6.2	800 <sup>+11</sup> <sub>-11</sub>	Maloof et al. (2006)
Laurentia	Gunbarrel dykes	B	248.7	44.8	138.2	9.1	12.0	778 <sup>+2</sup> <sub>-2</sub>	Calculation from Eyster et al. (2019) based on data of Harlan (1993); Harlan et al. (1997)
Laurentia-Svalbard	Svanbergfjellet Formation	B	18.0	78.5	226.8	25.9	5.8	770 <sup>+19</sup> <sub>-40</sub>	Maloof et al. (2006)
Laurentia	Uinta Mountain Group	B	250.7	40.8	161.3	0.8	4.7	760 <sup>+6</sup> <sub>-10</sub>	Weil et al. (2006)
Laurentia	Carbon Canyon	NR	248.2	36.1	166.0	-0.5	9.7	757 <sup>+7</sup> <sub>-7</sub>	Weil et al. (2004) as calculated in Eyster et al. (2019)
Laurentia	Carbon Butte/Awabubi	NR	248.5	35.2	163.8	14.2	3.5	751 <sup>+8</sup> <sub>-8</sub>	Eyster et al. (2019)
Laurentia	Franklin event grand mean	A	275.4	73.0	162.1	6.7	3.0	724 <sup>+3</sup> <sub>-3</sub>	Denyszyn et al. (2009a)
Laurentia	Long Range Dykes	B	303.3	53.7	175.3	-19.0	17.4	615 <sup>+2</sup> <sub>-2</sub>	Murthy et al. (1992)
Laurentia	Baie des Moutons complex (A)	B	301.0	50.8	152.7	-42.6	12.0	583 <sup>+2</sup> <sub>-2</sub>	McCausland et al. (2011)
Laurentia	Baie des Moutons complex (B)	B	301.0	50.8	141.5	34.2	15.4	583 <sup>+2</sup> <sub>-2</sub>	McCausland et al. (2011)
Laurentia	Callander Alkaline Complex	B	280.6	46.2	121.4	-46.3	6.0	575 <sup>+5</sup> <sub>-5</sub>	Symons and Chiasson (1991)
Laurentia	Catoctin Basalts	B	281.8	38.5	116.7	-42.0	17.5	572 <sup>+5</sup> <sub>-5</sub>	Meert et al. (1994)
Laurentia	Sept-Iles layered intrusion	B	293.5	50.2	141.0	20.0	6.7	565 <sup>+4</sup> <sub>-4</sub>	Tanczyk et al. (1987)